Interface Magnetism in Ferromagnetic Metal – Compound Semiconductor Hybrid Structures

Aidan T. Hindmarch
School of Physics & Astronomy, University of Nottingham, Nottingham, NG7 2RD, United Kingdom
aidan.hindmarch@nottingham.ac.uk

Interfaces between dissimilar materials present a wide range of fascinating physical phenomena. When a nanoscale thin-film of a ferromagnetic metal is deposited in intimate contact with a compound semiconductor, the properties of the interface exhibit a wealth of novel behaviour, having immense potential for technological application, and being of great interest from the perspective of fundamental physics. This article presents a review of recent advances in the field of interface magnetism in (001)-oriented ferromagnetic metal/III-V compound semiconductor hybrid structures. Until relatively recently, the majority of research in this area continued to concentrate almost exclusively on the prototypical epitaxial Fe/GaAs(001) system: now, a significant proportion of work has branched out from this theme, including ferromagnetic metal alloys, and other III-V compound semiconductors. After a general overview of the topic, and a review of the more recent literature, we discuss recent results where advances have been made in our understanding of the physics underpinning magnetic anisotropy in these systems: tailoring the terms contributing to the angular-dependent free-energy density by employing novel fabrication methods and ferromagnetic metal electrodes.

Keywords: Magnetic anisotropy, thin films and interfaces, III-V semiconductors

1. Introduction

Epitaxial growth of Fe on GaAs(001) was first reported, seemingly as an aside, in a paper on interface chemistry in Schottky contacts by Waldrop and Grant in 1979[1]. However, the curious and fascinating magnetic properties exhibited by epitaxial Fe/GaAs(001) systems were not revealed until 1983, when Jantz *et al.* mention, again almost in passing, a novel uniaxial magnetic anisotropy in thin Fe films on GaAs(001)[2]. This novel uniaxial anisotropy was finally placed firmly center-stage in 1987 by Krebs *et al.*[3]: this slow and steady build-up precipitated decades of intensive research into the properties of ferromagnetic films on the (001) surfaces of compound semiconductors — the topic of this review.

The Fe/GaAs(001) system is considered one of the original prototype systems in the field which has now come to be known as 'spintronics'[4]: Fe and GaAs are closely lattice matched, having lattice constants $d = 2.86$ Å and $a = 5.653$ Å respectively, allowing relatively easy cube-on-cube epitaxial growth, i.e., Fe(001)<100> || GaAs(001)<100>, with lattice mismatch of ~ 1.4 %. The interfaces between epitaxial bcc ferromagnetic metals and zincblende-structure semiconductors have been intensely studied not only because of their applicability to spintronics and unique magnetic anisotropy behavior, but also as they provide the ability to synthesize and characterize metastable crystalline phases of ferromagnetic metals. Here, we will cover recent advances in the field — an extremely comprehensive overview of the topic, as the state-of-the-art stood in 2005, has previously been provided by Wastlbauer and Bland[5]: we aim to focus on the more recent work, particularly with respect to magnetic anisotropies in these systems.

Whilst the microelectronics industry remains primarily focussed on silicon, compound semicon-

ductors are extensively used as test-bed and prototype systems in spintronics, in addition to having a great many applications in their own right. Ferromagnetic thin-films deposited on the III-V compound semiconductors attract the vast majority of interest: however, similar effects to those discussed here may also be observed in the zinc-blende II-VI compound semiconductors, one of the most frequently studied cases being ZnSe[4]. In recent years, the primary driving forces behind the continued interest in Fe/GaAs systems has been the quest for efficient injection of a spin-polarized current into a semiconductor. Currently, one of the more common device structures for spin-injection employs the Schottky barrier formed at the interface between an n-type semiconductor and ferromagnetic metal contact[6] in order to provide a 'tunnel' contact, negating the problem of conductivity mismatch[7] on the spin-injection efficiency. Although the principles of spin-injection apply equally to any semiconductor, GaAs and its related III-V compound semiconductors are particularly useful in this regard as a direct band-gap in the near-infra-red energy range, which may be easily modulated with III-V alloy composition, allows optical techniques to be employed. The spin-light-emitting-diode (spin-LED) structure[8] — consisting of a p-i-n quantum-well LED beneath a ferromagnetic contact, shown in figure 1a) — allows a model-independent, quantitative, determination of the carrier spin-polarization in the semiconductor from the circular polarization of the emitted electroluminescence[9].

Although planar devices such as the spin-LED have attracted significant research effort, in recent years attention has become increasingly focussed on lateral structures, aimed toward spintronic device implementations such as the now-infamous Datta-Das spin-field-effect-transistor (spin-FET)[10], shown in figure 1b). In the Datta-Das device, the spin-polarized current which flows in the semiconductor channel, often supposed as a 2-dimensional electron gas (2DEG), is manipulated by electrostatic gate-action, hence providing electrical control of the source-drain current in addition to that provided by the relative alignment of the ferromagnetic contacts. To this end, imaging of the injected spin-polarization from Fe into n-GaAs has been performed in a lateral geometry by Crooker *et al.*[11] and in a cross-sectional geometry by Kotissek *et al.*[12], whilst Lou *et al.*[13] and Lou *et al.*[14] have demonstrated all-electrical measurements of spin-injection, -transport and -detection in a single Fe/GaAs(001) device. Garlid *et al.*[15] have also used Fe/InGaAs(001) contacts to measure the transverse spin-current generated via the spin-Hall effect.

An interesting topic at present is magnetic tunnel junction structures, planar devices where a spin-polarized current tunnels between two ferromagnetic electrodes separated by a nanoscale insulating barrier layer, where the barrier is a compound semiconductor. Some theories predict very large tunnel magnetoresistance: the electronic-structure of the zincblende crystal makes 'coherent tunnelling' across the Fe/GaAs(001) interface possible[16]. Moser *et al.* fabricated Fe/GaAs/Fe(001) devices and find magnetoresistance around 6 % at 4.2 K, which reverses sign with increasing bias[17]: a result somewhat short of the 1000s of % change predicted. However, more recent theoretical work by Autès *et al.* has demonstrated that, due to the strong spin-orbit coupling in GaAs, saturation of the magnetoresistance is reached with increasing GaAs thickness, and a limited magnetoresistance (in the range as low as 30-50 %) results[18]. In the related magnetic tunnel transistor, a variant of the metal-base transistor structure with ferromagnetic metal emitter and base contacts, the ferromagnetic base acts as a hot-electron spin-filter, resulting in a highly spin-polarized current injected into the semiconductor collector[19]. Since the advent of crystalline ferromagnet/oxide/ferromagnet devices[20,21] it is now possible to fabricate fully epitaxial Fe/MgO/Fe/GaAs(001) transistor structures. Calculations by Autès *et al.* have demonstrated that the coherent crystal structure of these devices provides potentially very large magnetoresistive functionality[22], and the possibility of such spin-polarized resonant tunnelling devices has been shown by Nagahama *et al.*[23]. These results suggest potential for room-temperature operation of spin-transistor and spin-polarized resonant-tunnelling devices consisting solely of ferromagnetic metals and compound semiconductors.

One of the critical factors in enabling the technological application of nanomagnetism is that the magnetization direction in, for example, ferromagnetic spintronic storage and processing elements must be both stable and controllable. In order to bring this about, a complete understanding of the magnetic anisotropies in ferromagnetic thin films is of vital importance for future nanoscale spintronics applications: without such an understanding, a

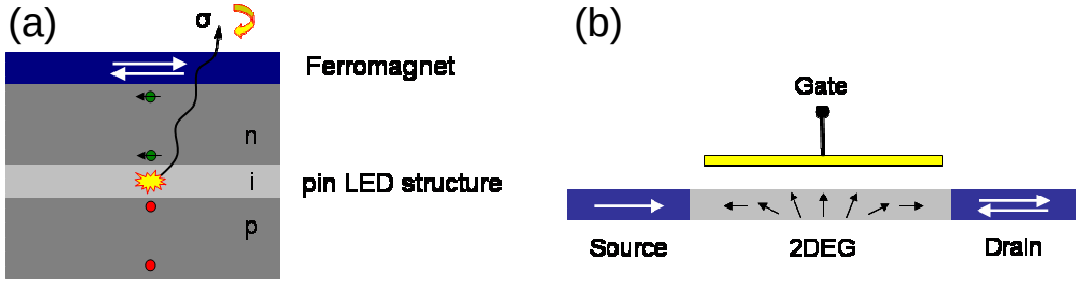

Fig. 1. Cartoon diagrams of (a) spin-LED and (b) Datta-Das spin-FET hybrid ferromagnet-semiconductor device structures.

fundamental limit is placed on the degree to which miniaturization of device elements may proceed. Thus, although the study of magnetic anisotropy has been reported for over a century[24], it still remains an important, pertinent, and interesting topic to this day.

2. Overview of magnetic anisotropies

The magnetic anisotropy energy is the difference in the Helmholtz free-energy for magnetization oriented along the 'easy'- and 'hard'-axes of the magnetic anisotropy: it provides the means by which the magnetization may be confined to lie along a given spatial direction and, along with the presence of a spontaneous magnetic moment, is crucial in producing ferromagnetism. In the absence of magnetic anisotropy, ordered moments are able only to access a superparamagnetic phase.

The magnetocrystalline anisotropy may be thought of as being related, via the spin-orbit interaction, to the anisotropy in the orbital magnetic moment associated with each lattice site. In Fe, Co, Ni, and their alloys, the 3d band is over half-filled; the spin-orbit coupling should restrict the maximal component of the orbital moment vector $\boldsymbol{m}_l$ to be parallel to the spin moment vector $\boldsymbol{m}_s$ (and hence magnetization). However, the crystal field interaction causes the orbital magnetic moment vector to be confined to a given high-symmetry direction[25] depending, in a non-trivial fashion, on factors such as the lattice spacing, orbital population etc.[26]. Provided the magnetization is aligned along such a high-symmetry direction of the cubic crystal, the free-energy of the system is minimized via the (leading) spin-orbit coupling term in the magnetic anisotropy energy, $\Delta E_{\mathrm{SO}} \propto -\boldsymbol{m}_l \cdot \boldsymbol{m}_s$[27]. Thus the magnetocrystalline anisotropy takes the same symmetry as the crystal lattice, and so bcc-ferromagnetic metals possess cubic magnetocrystalline anisotropy. One recalls that, in a bulk cubic crystal, the free-energy density ε is often expressed in terms of an expansion in powers of the direction cosines α_1, α_2 and α_3 which the magnetization makes with the crystal axes[28], giving

$$\varepsilon = K_1\left(\alpha_1^2\alpha_2^2 + \alpha_2^2\alpha_3^2 + \alpha_3^2\alpha_1^2\right) + K_2\alpha_1^2\alpha_2^2\alpha_3^2 + ..., \quad (1)$$

where K_1 and K_2 are the first- and second-order cubic magnetocrystalline anisotropy constants, respectively. (Typically $K_1 \gg K_2$, and K_2 is often taken to be zero: it is common also to neglect the isotropic term K_0 in the free-energy as it makes no overall contribution to the magnetic anisotropy energies).

2.1. *Cubic anisotropy in a ferromagnetic metal*

For the bcc crystal-structure, the three high-symmetry directions of the crystal $\langle 100\rangle$, $\langle 110\rangle$, and $\langle 111\rangle$, correspond to easy-, intermediate-, and hard-axes of the cubic magnetocrystalline anisotropy in Fe[28], corresponding to positive K_1 ($K_2 = 0$) in equation 1. In the bulk bcc-$\mathrm{Co}_x\mathrm{Fe}_{(100-x)}$ alloys (having stable bcc crystal structure for $x \lesssim 75$ at.%[29]) the sign of K_1 changes, corresponding to the cubic easy-axes shifting from the $\langle 100\rangle$ to the $\langle 111\rangle$ directions — and hence the cubic hard-axes from $\langle 111\rangle$ to $\langle 100\rangle$ — at compositions corresponding to around $x \sim 40$ at.%[28].

When the topic of discussion turns to thin-films, one must consider also the demagnetizing factor[30] due to shape-anisotropy, which causes the magnetization to preferentially lie in the plane of the layer: thus we need consider the $\langle 111\rangle$ directions no further as they do not lie within the plane of the (001)-oriented thin-film. The high-symmetry directions in the plane of the film are then the $\langle 100\rangle$ and $\langle 110\rangle$ directions, which for Fe are thus the *in-plane* cubic easy- and hard-axes, respectively.

Table 1. Summary of the in-plane easy- and hard-axis directions of the cubic magnetocrystalline anisotropy for epitaxial body-centered cubic thin-films of the ferromagnetic 3*d* transition-metals and their alloys, deposited on GaAs(001).

Material	Composition range	Cubic easy-axes	Cubic hard-axes	Reference
Fe	—	[100], [010]	[110], [1$\bar{1}$0]	5
$Co_xFe_{(100-x)}$	$x \lesssim 30$ %	[100], [010]	[110], [1$\bar{1}$0]	31
$Co_xFe_{(100-x)}$	$30 \lesssim x \lesssim 70$ %	[110], [1$\bar{1}$0]	[100], [010]	32, 31, 33, 34
Co	—	[100], [010]	[110], [1$\bar{1}$0]	35, 36
Ni	—	[100], [010]	[110], [1$\bar{1}$0]	37
$Ni_xFe_{(100-x)}$	all x	[100], [010]	[110], [1$\bar{1}$0]	38

Table 1 shows the easy- and hard-axis directions of the cubic magnetocrystalline anisotropy for thin-films of various ferromagnetic metals on GaAs(001): in each case the ferromagnet has a bcc crystal structure, which is a metastable phase for many of these materials. An interesting, and somewhat surprising, result is found: in almost all cases, the exception being the 'Co-rich' CoFe alloys, the cubic magnetocrystalline anisotropy has easy axes along the in-plane $\langle 100 \rangle$ directions[31,35–38] — as is expected for Fe. This is despite the fact that in their stable fcc crystal phases, both Co and Ni have cubic easy-axes along the $\langle 110 \rangle$, i.e., K_1 is expected to be negative[28]. In $Co_xFe_{(100-x)}$, the cubic anisotropy constant indeed changes sign, becoming negative for $x \gtrsim 30$ at.%[31,32]: however, studies in the composition range $70 \lesssim x < 100$ at.%, where it appears a further sign-reversal must occur, have not yet been performed. In the case of the $Ni_xFe_{(100-x)}$ alloys the cubic anisotropy constant is again positive, with in-plane cubic easy-axes along $\langle 100 \rangle$ directions, over the entire composition range: in these alloys, though, the magnetocrystalline anisotropy becomes vanishingly small over a wide composition range, $20 < x < 80$ at.%[38], despite both bcc-Fe and Ni having large, positive K_1 in elemental form. The supposedly well-understood magnetocrystalline anisotropy reveals some surprising results in these materials.

The first experimental work focussing solely on magnetism in epitaxial Fe films on GaAs(001) was reported in 1987 by Krebs *et al.*[3]. Their ferromagnetic resonance measurements indicated that whilst the free-energy density for magnetizing the film along the in-plane $\langle 100 \rangle$ directions were equivalent, due to the anticipated cubic magnetocrystalline anisotropy in their Fe films, the in-plane $\langle 110 \rangle$ directions were inequivalent — indicative of an additional *uniaxial* magnetic anisotropy term K_U with easy-axis oriented along the [110] and hard-axis along the [1$\bar{1}$0] direction. The origin of this *uniaxial* magnetic anisotropy which is found in these, and related, films has escaped explanation: it is toward gaining an understanding of this anisotropy we will focus the remainder of this review.

2.2. *Mixed cubic and uniaxial magnetic anisotropy*

In thin-film magnetism, the 'effective' anisotropy constants are frequently considered to be composed of a combination of volume and interface terms, which may be explicitly separated in the form

$$K_a^{eff} = K_a^{vol} + K_a^{int}/t, \tag{2}$$

where a = U, 1, 2, etc., and t is the thickness of the ferromagnetic film. For thin epitaxial bcc-ferromagnet/III-V(001) one typically finds $K_U^{vol} \approx 0$ and $|K_1^{vol}| \gg |K_1^{int}|$. Thus the uniaxial magnetic anisotropy is purely interfacial in origin, related in some way to the interface between the ferromagnetic metal film and the compound semiconductor.

The cubic magnetocrystalline anisotropy arises predominantly due to the film volume, and has only a weak thickness dependence due to truncation of the crystal lattice symmetry at the interface. This truncation of the lattice results in an interfacial component to the cubic anisotropy of opposite sign to the volume component: at a critical thickness, typically found to be around 6 monolayers (ML)[39], the interface term dominates and the effective cubic anisotropy K_1^{eff} changes sign — the easy axes of the cubic magnetocrystalline anisotropy rotate from, e.g., $\langle 100 \rangle$ to $\langle 110 \rangle$ directions for Fe. Note that this effect is purely related to loss of translational symmetry in the bcc lattice of the ferromag-

netic film: the use of different substrate materials has negligible further influence on the cubic magnetocrystalline anisotropy.

In the prototypical epitaxial bcc-Fe/GaAs(001) system, within the Stoner-Wohlfarth model[40] of coherent magnetization reversal by rotation of a single domain, one may rewrite equation 1 to express the angular-dependence of the free-energy density including terms describing magnetocrystalline, magnetoelastic, interface, and Zeeman energy terms for saturation magnetization $M_{\rm S}$ making an angle θ with the in-plane [100] direction as[41]

$$\begin{aligned}\varepsilon(\theta) \quad &\sim \tfrac{K_1^{\rm eff}}{4}\sin^2(2\theta) + \tfrac{B_2\epsilon}{2}\sin^2(2\theta) \\ &+\tfrac{K_{\rm U}^{\rm int}}{t}\sin^2\left(\theta-\tfrac{\pi}{4}\right) - HM_{\rm S}\cos(\theta), \end{aligned} \quad (3)$$

where B_2 is the second order magnetoelastic coupling constant, and ϵ the shear strain. Although there is a lattice mismatch of around 1.4 % between Fe and GaAs, it is common for the magnetoelastic term to be omitted from the analysis of anisotropies in Fe/GaAs(001) contacts. For $Co_xFe_{(100-x)}$ alloys the magnetocrystalline anisotropy constant changes sign at $x \sim 30-45$ %[28,31]: hence whilst equation 3 remains appropriate for Fe-rich alloys, a more appropriate expression for the free-energy density in Co-rich alloys on GaAs(001) is commonly written (omitting the magnetoelastic term) as[32]

$$\begin{aligned}\varepsilon(\phi) \sim &-\tfrac{K_1^{\rm eff}}{4}\sin^2(2\phi) + \tfrac{K_{\rm U}^{\rm int}}{t}\sin^2(\phi) \\ &-HM_{\rm S}\cos(\phi-\alpha), \end{aligned} \quad (4)$$

where now ϕ is the angle between the magnetization and the [110] direction, and α is the angle between H and the [110] direction. It is obvious that care must be taken in applying the correct expression: further difficulties may arise when the interfacial uniaxial easy axis is no-longer oriented along the [110] direction, but rather along $[1\bar{1}0]$, as is the case in films deposited on, for example, InAs(001).

When considering such an admixture of cubic magnetocrystalline and interfacial uniaxial magnetic anisotropies, three distinct situations may occur: i) when the ferromagnetic film is very thick, in which case $|K_{\rm U}^{\rm eff}| \ll |K_1^{\rm eff}|$, the uniaxial anisotropy is negligible and the film behaves as if it has only cubic in-plane magnetic anisotropy; ii) in the case when the ferromagnetic film is very thin, in which case $|K_{\rm U}^{\rm eff}| \gg |K_1^{\rm eff}|$, the cubic anisotropy is negligible and the film behaves as if it has only uniaxial in-plane magnetic anisotropy; and, iii) when the film is of a thickness where $|K_{\rm U}^{\rm eff}| \approx |K_1^{\rm eff}|$, both terms contribute, which results in two-stage magnetization reversal for fields applied along the uniaxial hard-axis (UHA), depicted schematically in the inset to the lower right frame of figure 2. Straight arrow represents a coherent rotation of the magnetization, whilst curved arrows represent abrupt changes in magnetization direction. The strength of the uniaxial magnetic anisotropy determines the points at which the magnetization jumps between the uniaxial hard-axis and cubic easy axis (CEA).

2.3. *Evaluation and quantification of the anisotropy*

Where the uniaxial magnetic anisotropy dominates, $M(H)$ is single-valued (figure 2, lower left): we may obtain an expression for $H(m)$, where the normalized magnetization component along the uniaxial hard-axis is $m = M/M_{\rm S} = \sin\theta$, from minimizing equation 4 for $\alpha = \pi/2$, i.e., field applied along the uniaxial hard-axis. In this case the anisotropy constants may simply be evaluated by fitting

$$H(m) = 2K_1^{\rm eff}\left(2m^3 - m\right)/M_{\rm S} + 2K_U^{\rm eff}m/M_{\rm S}. \quad (5)$$

In cases where a two-stage magnetization-reversal is observed, following the method outlined by Dumm *et al.*[32] we are able to extract the effective uniaxial anisotropy constant $K_{\rm U}^{\rm eff}$ and first order effective cubic anisotropy constant $K_1^{\rm eff}$ from the hysteresis loops measured along the UHA, figure 2 lower right, assuming that the magnetization reversal around zero applied field takes place by a coherent rotation. It may be shown that the effective anisotropy constants are given by

$$K_{\rm U}^{\rm eff} = -\frac{1}{2}\frac{M_{\rm S}H_{\rm S}\left(H_{\rm S}^2s^2 + H_{\rm S}s + 2\right)}{H_{\rm S}^3s^3 + H_{\rm S}^2s^2 + H_{\rm S}s + 1} \quad (6)$$

and

$$K_1^{\rm eff} = -\frac{1}{2}\frac{M_{\rm S}\left(H_{\rm S}s - 1\right)}{\left(H_{\rm S}^3s^3 + H_{\rm S}^2s^2 + H_{\rm S}s + 1\right)s}, \quad (7)$$

where $H_{\rm S}$ and s are respectively the shift-field and zero-field slope of the normalized hysteresis loops, as indicated in figure 2[33,34]. Thus extraction of both the uniaxial and cubic anisotropy constants may be readily achieved across the whole thickness range using simple hysteresis loop measurements. More complicated experimental techniques, including ferromagnetic resonance and Brillouin light scattering, have also been extensively applied to these systems in order to extract the magnetic anisotropy

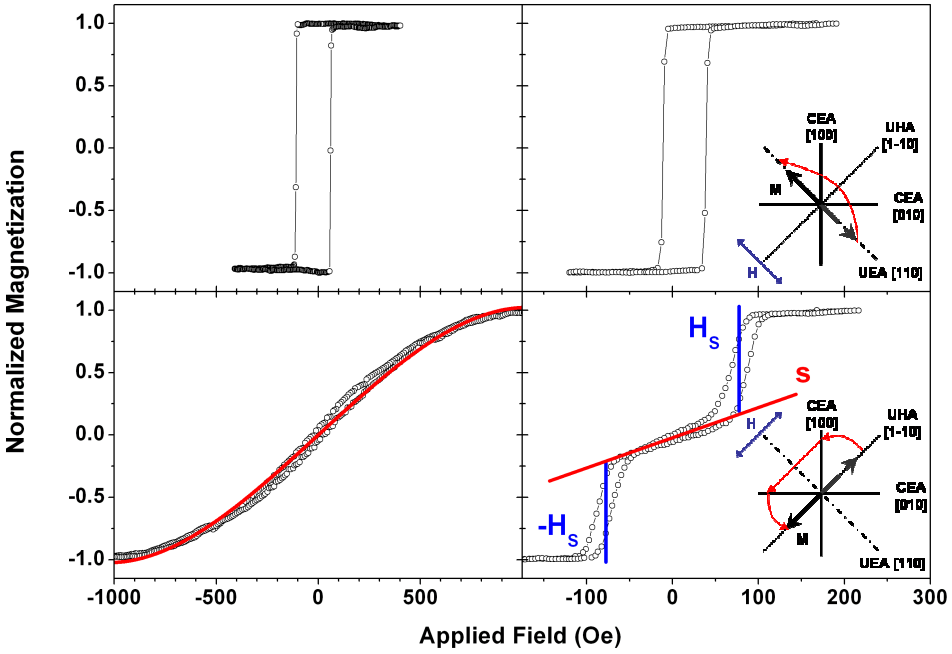

Fig. 2. In-plane magneto-optic Kerr effect hysteresis loops for $Co_{70}Fe_{30}$/GaAs(001) along (upper) the uniaxial easy-axis and (lower) the uniaxial hard-axis. Left frames are an ultra-thin film, where the uniaxial magnetic anisotropy dominates, and right frames are a slightly thicker film, where uniaxial and cubic magnetic anisotropies are of similar strength. Shown inset on the right are schematics showing an example of the in-plane magnetic anisotropy and magnetization reversal. The lower left frame shows a fit to the hysteresis data using equation 5, and in the lower-right frame the zero-field slope s and split-field H_s features, which may be used in determining the magnetic anisotropies from equations 6 and 7, are indicated. (After Hindmarch *et al.*[34].)

Table 2. Summary of lattice mismatch between Fe and various III-V compound semiconductors (and the II-VI compound ZnSe), valence spin-orbit parameter in the semiconductor, and the direction of the interface-induced uniaxial easy-axis for an Fe thin-film deposited onto the (001) surface.

Material	Lattice const. a (Å)	Lattice mismatch η (%)	S-O coupling Δ_0 (eV) [a,b]	UEA	References
GaAs	5.65	1.41	0.34	[110]	42, 43, 44
$Al_8Ga_{92}As$	—	—	~ 0.33	[110]	45
AlAs	5.66	1.25	0.3	[110]	46
$In_{20}Ga_{80}As$	—	0	~ 0.33	[110]	42
$In_{50}Ga_{50}As$	—	−2.13	~ 0.33	[110]	44, 47 (IBD)
$Al_{48}In_{52}As$	—	(−)2.2	—	[110]	48
InP	5.87	−2.32	0.11	$[1\bar{1}0]$	49
InAs	6.06	−5.37	0.38	$[1\bar{1}0]$	50, 42
GaSb	6.09	−5.95	0.76	—	46
ZnSe	5.67	1.14	0.43 [c]	[110]	51

Note: [a] Values for the valence spin-orbit parameter in the binary III-Vs taken from reference 52.
[b] Values for the valence spin-orbit parameter in the ternary III-Vs after reference 53.
[c] Value for the valence spin-orbit parameter in ZnSe taken from reference 54.

constants: very good agreement is found between the results for different techniques. As an experimentalist there is now a collection of tools which are suitable for studying magnetism in ferromagnet-semiconductor hybrid structures.

3. Influence of the underlying compound semiconductor

As we have seen, the cubic magnetocrystalline anisotropy is strongly dependent on details of the ferromagnetic metal film, particularly its elemen-

tal composition and thickness: the uniaxial magnetic anisotropy, on the other hand, seems relatively robust against changes to the ferromagnetic metal film. The crystallographic direction along which the uniaxial easy-axis lies is also dependent on the material constituents of the contact: however, in this case it is the *semiconductor* which determines the uniaxial anisotropy, rather than the ferromagnet.

Values for the lattice constant a, lattice mismatch $\eta = (a - a_{\mathrm{Fe}})/a$, valence spin-orbit coupling strength Δ_0, and the interface induced uniaxial easy-axis direction for various epitaxial Fe/III-V(001) systems (and Fe/ZnSe(001)) are given in table 2. Entries for the III-Vs are ordered by increasing lattice parameter, and we see that the lattice mismatch for the epitaxial Fe overlayer passes through a minimum, being roughly zero for the $In_{20}Ga_{80}As$ ternary compound. One very interesting point to note is the dependence of the uniaxial easy-axis direction on the lattice mismatch: if one were to assume that the interface anisotropy arises due to epitaxial strain or anisotropic stress relaxation, as have previously been suggested in the literature, one may think that a positive lattice mismatch ($2a_{\mathrm{Fe}} > a$) results in interface anisotropy along [110]. From this, we would then anticipate the interface anisotropy vanishing when the lattice mismatch is zero — leaving only the cubic magnetocrystalline anisotropy: however, this is not the case[42]. Indeed, for both $In_{50}Ga_{50}As$ and $Al_{48}In_{52}As$ ternary compounds, the lattice mismatch is *negative* ($2a_{\mathrm{Fe}} < a$) but the easy-axis of the uniaxial magnetic anisotropy remains along the [110] direction. This shows that it is unlikely that epitaxial strain is the origin of the uniaxial interface anisotropy, as is now the generally-held consensus[33,41,55,56].

An additional point to note is the variation of the valence-band spin-orbit splitting parameter, a measure of the spin-orbit interaction strength in the semiconductor. In most of the III-V materials it is in the range 0.3–0.4 eV, with the specific exceptions of InP and GaSb. In GaSb the spin-orbit interaction is far stronger, mainly due to the 'heavy' antimony, but, due to the large lattice mismatch with Fe, defect-free epitaxial growth is difficult and the uniaxial magnetic anisotropy has not been observed in this system. However, in InP the spin-orbit interaction strength is much smaller than in the other III-Vs: in reference 49, Zakeri *et al.* found that the uniaxial magnetic anisotropy in Fe/InP(001) not only is rotated 90° relative to that in Fe/GaAs(001), but also is significantly weaker.

Given the dependence of the uniaxial magnetic anisotropy on the underlying semiconductor material, the influence of the capping layer material has also been investigated; particularly the influence on the in-plane uniaxial magnetic anisotropy. Shaw *et al.* have found that an Al capping can induce a volume component to the uniaxial anisotropy in ultra-thin Fe films on GaAs(001), and suggest that this may be due to an additional anisotropic strain mechanism which is absent for Au or Cu capping. Morley *et al.* observe slight differences between Cr and Au capping of Fe films on GaAs(001) and InGaAs(001), concluding that the primary mechanism for the effect is additional interdiffusion at the Cr/Fe interface over the Au/Fe interface[44].

A further mechanism which has been shown to cause a modification of the uniaxial magnetic anisotropy in epitaxial films are surface step-edges. Epitaxial CoFe films deposited on vicinal GaAs(001) substrates, miscut at various angles towards the two inequivalent [111] planes, have been studied by Isakovic *et al.* and Wolf *et al.*. In both cases a rock-salt structured $Sc_{30}Er_{70}As$ buffer layer has been deposited between GaAs(001) and CoFe: the buffer-layer acts to weaken the interfacial uniaxial magnetic anisotropy, making the the influence of the substrate miscut more clearly apparent. The substrate miscut is found to influence the reversal path taken by the magnetization, allowing the vector magnetization response of the film to an applied magnetic field to be tailored[57,58]. Yoo *et al.* have studied Fe films deposited onto a range of vicinal GaAs(001) surfaces[59], and shown that an asymmetric planar Hall effect arises due to the magnetization reversal occurring in the (001) plane rather than the (vicinal) plane of the film.

In a similar fashion to, for example, the exchange-bias effect, the unique magnetic anisotropies which arise if hybrid ferromagnet-semiconductor systems are now beginning to be utilized as a means to control the magnetic anisotropy in nanoscale systems, in addition to being a stand-alone topic of study. Kipferl *et al.* compared the 'Bloch-3/2 law' spin-wave parameters[30] for Fe films epitaxially deposited on GaAs(001) and Au(001), finding a smaller depolarization due to thermal spin-waves in Fe/GaAs(001) as a consequence of the additional magnetic anisotropy contribution from the interfacial uniaxial magnetic anisotropy[60].

Kipferl *et al.* and Niu *et al.* have both investigated magnetic properties of arrays of sub-micron epitaxial Fe dots patterned on GaAs(001)[61,62]. Niu *et al.* find that using a focussed ion-beam milling technique to pattern the dot-array appears to cause modifications to the magnetic anisotropies. Meng *et al.* have demonstrated the interplay between cubic magnetocrystalline, interface-induced uniaxial, and shape anisotropies in a series of arrays of micron-scale rectangular elements[63]. Despite extensive use being made of the ferromagnet/semiconductor interface-induced uniaxial magnetic anisotropy, the details of the origin of the effect are still not well understood.

3.1. *What may determine the uniaxial magnetic anisotropy?*

Since the initial work of Jantz *et al.* and Krebs *et al.* on magnetism in Fe/GaAs(001), the field has expanded to an unprecedented extent: hybrid ferromagnet-semiconductor structures and devices are now key topics in nanomagnetism and spintronics. However, despite extensive study extending over more than a quarter of a century, the physical origin of the interfacial uniaxial magnetic anisotropy in these systems has continued to retain something of an air of mystery. From early work in the field, several ideas as to how the uniaxial anisotropy arises have been put forward, each of which seems to have found favour for at least a short period of time. Below we briefly summarize the areas which have been studied previously, and how these have been shown to contribute (or not) to the interfacial induced uniaxial magnetic anisotropy.

Direction of the uniaxial magnetic anisotropy: In the early literature on the subject there is significant disagreement over exactly which crystallographic direction corresponds to the uniaxial easy axis: although in some of the first reported cases the uniaxial easy-axis was not well defined (most probably as a result of poorer interface quality in the earlier works), later reports appeared to disagree on whether the uniaxial easy-axis was aligned along [110] or [1$\bar{1}$0]. Wastlbauer and Bland reanalyzed the prior literature on the subject and concluded that, after correcting for accidentally misreported crystallographic axes, the uniaxial easy-axis in Fe/GaAs(001) is oriented along the [110] direction, with the uniaxial hard-axis along [1$\bar{1}$0][5].

Anisotropic island-growth: Numerous studies on the initial stages of growth of Fe on GaAs(001) have found that the growth proceeds initally as a 3-D island growth mode, with islands nucleating along the As dimer rows ([1$\bar{1}$0] direction). These Fe islands then gradually coalesce as the coverage increases, with islands elongating along [1$\bar{1}$0], and average height in the range 1–2 ML[64,65]. Coalescence generally occurs at nominal thickness of around 2–3 ML[66]; while well-separated islands are observed, the surrounding areas of the GaAs(001) surface are found typically to retain their initial surface reconstruction. Although the interface structure beneath the Fe islands is unknown, Ionescu *et al.* have proposed a model of Fe_2As cluster formation during the initial stages of growth[65], and Godde *et al.* found clusters of both Fe_2As and $Fe_3Ga_{(2-x)}As_x$ following thermal processing[67]. Gillingham *et al.* showed that Fe islands may relax by anisotropic diffusion, favouring [1$\bar{1}$0], over a period of $\sim$ 30 hours[66]. However, Thomas *et al.* demonstrated that the shape-anisotropy due to elongated grain-growth in Fe/GaAs(001) does *not* influence the uniaxial magnetic anisotropy[41].

Magnetoelastic coupling: Related to the above discussion of island-growth during early stages of film deposition, it has been suggested that anisotropic epitaxial strain, and/or anisotropic stress relaxation may determine the interfacial uniaxial magnetic anisotropy, e.g., from first-principles calculations by Mirbt *et al.*[68]. Thomas *et al.* also found that anisotropic shear-strain has no influence on the uniaxial magnetic anisotropy in their Fe/GaAs(001) films[41]. It is now considered, in-part also due to observations of strong uniaxial magnetic anisotropy in CoFe/GaAs(001) systems with far lower lattice mismatch than Fe/GaAs[31–34], that whilst magnetoelastic coupling *may* contribute to the interfacial uniaxial magnetic anisotropy, it must play only a relatively minor rôle.

Interface bonding: The idea that the uniaxial magnetic anisotropy in Fe/GaAs(001) was in some way related to interfacial bonding was first suggested by Jantz *et al.*, who supposed that the lack of four-fold symmetry could perhaps be reconciled by considering that the GaAs(001) surface presented a reduced symmetry, possibly due to surface reconstruction[2]. Several years later, Krebs *et al.* astutely commented that the dangling bonds at an unrecon-

structed GaAs(001) surface reduced the in-plane symmetry. If the surface is Ga-terminated then the two unsatisfied tetrahedral bonds per surface atom are oriented along [110], whilst for an As-terminated surface they are oriented along [1$\bar{1}$0]: this breaking of the in-plane four-fold symmetry at the surface may provide an indirect means by which the uniaxial magnetic anisotropy may form[3]. Freeland *et al.* demonstrated modifications to the interfacial electronic structure in Fe/GaAs(001): they found a significant charge-transfer from Fe to GaAs(001) due to interfacial bonding, and, based on the relative electronegativities of Fe, Ga, and As, concluded that an Fe-As bonding configuration is dominant at the interface[69]. These Fe-As bonds will preferentially form along the [1$\bar{1}$0] direction, as suggested by Krebs *et al.*, in order to preserve the tetrahedral bonding symmetry: Freeland *et al.* suggested that this may be the origin of the interfacial uniaxial magnetic anisotropy in Fe/GaAs(001), an idea which is accepted by many.

Semiconductor surface reconstruction: A range of studies using various reconstructions of the GaAs(001) surface have demonstrated the presence of a uniaxial magnetic anisotropy[5]. Whilst the idea that As-dimers running along the [1$\bar{1}$0] direction of the reconstructed GaAs surface break the in-plane cubic symmetry and provide anisotropic interfacial bonding coordination has been extensively put forward as an explanation for the uniaxial magnetic anisotropy, Kneedler *et al.*[64], and later Moosbüler *et al.*[70], have clearly demonstrated that the reconstruction of the GaAs(001) surface prior to depositing Fe makes no discernible difference to the uniaxial magnetic anisotropy.

It is concluded that, whilst the initial growth of ferromagnetic films on GaAs(001) is an interesting and important topic in itself, it seems that these studies are unable to shed light on the origins of the uniaxial magnetic anisotropy. Similarly those investigations into the reconstruction of the semiconductor surface prior to ferromagnetic film growth, which again show little influence on the uniaxial anisotropy. The influence of epitaxial strain in systems with large lattice mismatch appears to be to reduce the uniaxial anisotropy: however, epitaxial strain does not seem to be the mechanism which causes the anisotropy to appear in the first-place. Finally, the anisotropic interface bonding, for example between Fe and As, which was initially proposed as a potential mechanism for the anisotropy, still holds the strongest claim to be the 'cause' of the magnetic anisotropy. It seems very likely that the Fe-As interfacial bonding is responsible for the *direction* of the uniaxial interface anisotropy: what exactly determines the strength of the uniaxial magnetic anisotropy is, at this point in time, still an open question.

3.2. *Theory and modelling of hybrid structures*

The interfacial magnetic anisotropy in ferromagnet/III-V(001) systems is one of the few areas of modern nanoscience where experimental findings are only very loosely guided by theory (at least from the perspective of an experimentalist!). Whilst the ability to fabricate and characterize these types of structure has rapidly emerged, the theoretical tools required for truly *ab-initio* theoretical investigations are still lacking at present. Magnetocrystalline anisotropy energies are usually calculated by applying the 'torque theorem', whereby the electronic structure and total energy is calculated for unconstrained magnetization, producing the result for magnetization along the easy-axis, then the magnetization is constrained to lie along the hard axis and the total energy re-minimized. The magnetic anisotropy energy is the (small) difference between the (large) total energies for magnetization along hard- and easy-axes. Due to the fact that one must calculate the total energies to high precision in order to obtain an accurate value of the anisotropy energy, until the advent of fairly recent computational advances it was not possible to accurately predict the sign, never mind the magnitude, of the magnetic anisotropy energy from first-principles — even in an elemental metal.

To further complicate matters, as we are interested in a hybrid structure, one requires a method which is able, at the same time, to accurately model the electronic structure of both a ferromagnetic metal *and* a compound semiconductor. Success has been achieved by using parameterized models, for example tight-binding, where the parameters for both metals and semiconductors are well-known. Košuth *et al.* obtained reasonably good agreement with experimental results for Fe/GaAs(001) using a tight-binding Korringa-Kohn-Rostoker method with spin-orbit interaction, assuming an ideal Fe/GaAs(001) interface[55], and

attribute the anisotropy to interfacial Fe-As bonding. Sjöstedt *et al.* studied Fe/ZnSe(001) using an *ab-initio* full-potential linearized augmented-plane-wave method, finding that epitaxial strain is not required for uniaxial magnetic anisotropy to be present, and that the spin-orbit coupling at the interfacial Fe sites is important in realizing uniaxial magnetic anisotropy[71]. Until fairly recently, theoretical calculations have 'only' been able to suggest mechanisms which may (or may not) be important in determining the uniaxial magnetic anisotropy: the increased computing power available means that modelling of this type of hybrid system is now rapidly approaching the point where quantitative predictions may be made.

4. Advances in fabrication and characterization

Having given an overview of the topic and discussed the magnetic anisotropies which arise in ferromagnetic films on III-V semiconductors, we now go on to discuss some of the more important recent advances in the field, with the particular aim of clarifying the physical mechanisms which underpin the interface-induced uniaxial magnetic anisotropy.

4.1. *Fabrication of hybrid structures*

Until fairly recently the only method which had been employed extensively in fabricating ferromagnet/semiconductor hybrid contacts was molecular beam epitaxy (MBE): although this technique results in extremely high-quality device structures, in recent years there has been increasing interest in forming epitaxial ferromagnetic films onto semiconductor surfaces by other means, which may be less costly and allow higher throughput. However, before discussing film-deposition techniques, it seems pertinent to describe the preparation of a smooth, ordered, semiconductor surface on which to deposit.

4.1.1. *Semiconductor surface preparation*

As discussed above, there is a great deal of information suggesting that the exact nature of the surface reconstruction plays little role in determining the magnetic anisotropies of the ferromagnetic film: however, preparation of a smooth, clean, semiconductor surface onto which the ferromagnetic films may be grown is of critical importance. Here we will summarise some of the wide range of surface-preparation protocols which have been employed: further details of the surface reconstructions of GaAs(001) may be found in reference 5.

The ideal method of fabricating a ferromagnet/semiconductor contact would involve growing a semiconductor epilayer in a dedicated III-V MBE system, with subsequent ferromagnetic metal film growth either in the same vacuum chamber or following a short in-vacuum transfer to a separate metal-growth chamber. Using III-V MBE, formation of a given termination and surface reconstruction may be readily achieved through regulation of the substrate temperature and As flux after depositing the semiconductor epilayer[64,72]. These procedures have been used successfully by some groups[9,72,73]: unfortunately, such combinations of coupled III-V and metal deposition facilities are not always available, and so other surface preparation schemes are often employed.

One alternate method is to grow a III-V epilayer by MBE and then passivate the surface with an amorphous As capping layer, which protects the semiconductor surface from oxidation during transfer through atmosphere. Once back under vacuum, the wafer is heated in order to thermally desorb the As passivation, leaving a clean semiconductor surface on which to deposit metal[48,66,74]: desorption of the As passivation typically occurs at temperatures in the region of 450 °C. This method of obtaining a clean III-V surface is particularly common where sputter-deposition of the ferromagnetic metal is employed[34,56,75,76]: as these types of deposition system generally lack surface analysis tools, little is known regarding the phase of the surface reconstructions achieved. Further surface treatment may also be applied, typically in the form of an *in-situ* thermal anneal of the As-desorbed wafer. For example, heating to 560 °C for 60 mins has been shown to result in a GaAs(001)-(2×4) reconstructed surface[42]. We note that there are, in-fact, several distinct surface reconstructions that are described as (2×4), see reference 5 for further details.

By far the most popular technique for achieving a clean semiconductor surface involves using *in-situ* etch and anneal processes on commercial epi-ready III-V wafers. This has the obvious benefit with regard to cost, as a commercial epi-ready wafers are significantly cheaper than MBE-grown epilayers. Using such an etch-anneal procedure, by far the most commonly reported surface is the GaAs(001)-

(4×6) reconstruction. This is formed by processes involving annealing in the region of 600 °C, whilst bombarding the surface with 0.5-1 keV Ar^+-ions for a period of between 30–80 mins[32,37,43,77] — a somewhat broad range of process parameters. In some cases multiple flash-anneal steps are also included[78,79]. Reconstructions termed '(4×6)' are, more correctly, in fact a combination of regions of (4×2) and (2×6) reconstructed surface phases[66,80], i.e., the surface reconstruction is properly termed the GaAs(001)-$(4 \times 2)/(2 \times 6)^5$. This perhaps explains the relative ease in achieving such a surface reconstruction.

Single-phase surface reconstructions may be achieved using similar etch-anneal parameters. Godde *et al.* have shown that, following an initial surface etch with 0.5 keV Ar^+-ions for 45 mins at room-temperature, annealing at 500 °C for a further 45 mins results in the GaAs(001)-(2×6) reconstructed surface, whilst annealing at 600 °C results in the GaAs(001)-(4×2) surface phase[67]. Lee *et al.* showed that, following an unspecified initial etch-anneal cycle, a final anneal at 570 °C for 30 mins also produces the GaAs(001)-(4×2) reconstruction[81]. In an earlier study by Moosbühler *et al.*, an initial etch-anneal for 30 mins at 600 °C with 1 keV Ar^+-ion bombardment, then followed by 5 mins at 600 °C, with 0.5 keV Ar^+-ion bombardment resulted in the GaAs(001)-(2×4) surface, whilst 5 mins at 500 °C, 0.5 keV Ar^+ produced GaAs(001)-(2×6)[70].

We note in passing that the GaAs(110) surface does not have the rich variety of interface terminations and reconstructions which may be observed in the case of GaAs(001) — in-fact, due to its non-polar nature, the GaAs(110) has only the trivial (1×1) reconstruction (with slight relaxation of the surface-layer bond angles) and forms a natural cleavage-plane of the zinc-blende crystal lattice. Whilst formation of a clean, oxide-free, semiconductor surface is critical both to the epitaxial growth of the FM metal overlayer and overall quality of the deposited structure, as discussed by Kneedler *et al.* and Moosbühler *et al.*, the magnetic anisotropy in an Fe film is independent of the GaAs(001) surface reconstruction onto which it is deposited. Thus, knowledge of the exact nature of the semiconductor surface reconstruction/composition is of less significance than had initially been suggested. However, details of the film growth are often of importance in determining the interface properties.

4.1.2. *Ferromagnet film deposition*

Since the original inception of ferromagnet/semiconductor hybrid contacts, the growth method of choice for the ferromagnetic metal has been MBE. Deposition of the ferromagnetic metal from either an electron-beam hearth or thermal evaporation (Knudsen) cell typically results in growth rates of the order of 1 ML/min ($\sim$ 0.05 Å/s) and produced extremely high-quality epitaxial single crystalline films.

In recent years, alternative methods for depositing epitaxial ferromagnet contacts onto semiconductors have begun to be explored. One major driving factor behind this is the fact that MBE growth is both expensive and time-consuming; consequently making this technique unattractive for industrial application. Ion-beam sputter deposition has been used for epitaxial growth of Fe on GaAs(001), by Damm *et al.*[82], and on InGaAs(001) by Richomme *et al.*[47], and in both cases the structural quality of the films, in addition to the magnetic anisotropies, are found to be comparable to those obtained in the respective MBE-grown systems.

Formation of epitaxial Fe contacts to GaAs(001), GaAs(110), and GaAs(111) from a ferrous ammonium sulphate ($Fe(NH_4)_2SO_4$) electrolytic solution by Bao *et al.*[83], and a comparison between contacts to GaAs(001) using iron chloride ($FeCl_2$) and ferrous ammonium sulphate electrolytes by Svedberg *et al.*[84], have demonstrated that electrodeposition may also be a useful technique for ferromagnet/semiconductor contact formation. As electrodeposition is a very low-energy method, the formation of very abrupt interfaces should be possible by this technique[84]. Low-pressure metal organic chemical vapour deposition (LP-MOCVD) has also been successfully used by Liu *et al.* to fabricate epitaxial Fe films on GaAs(001)[85].

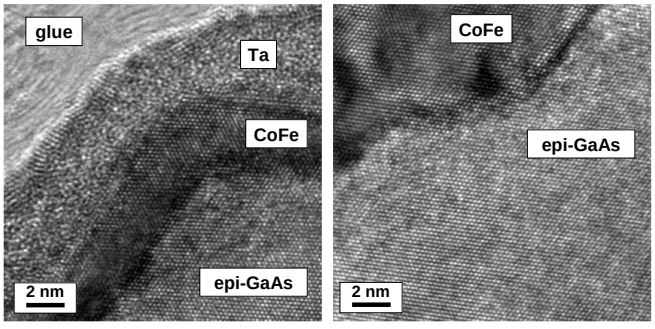

Fig. 3. Cross-sectional transition electron micrographs of Ta[25 Å]/$Co_{70}Fe_{30}$[35 Å] and Ta[25 Å]/$Co_{70}Fe_{30}$[1100 Å]

films on GaAs(110), viewed along the GaAs⟨111⟩ zone axis: the scale bars are 2 nm. The $Co_{70}Fe_{30}$ film grows coherently on GaAs(110), despite the large surface features, and the coherent crystal structure extends through the film thickness. (After Hindmarch *et al.*[86].)

Magnetron sputter deposition of epitaxial $Co_{70}Fe_{30}$ films on GaAs(001)[34,87] and GaAs(110)[86] has been demonstrated by Hindmarch *et al.*: the very small lattice mismatch between $Co_{70}Fe_{30}$ and GaAs allows a relatively high deposition rate of ~ 2 Å/s to be used, with no formation of secondary crystal phases in $Co_{70}Fe_{30}$ films over $\sim$ 100 nm thick: figure 3 shows a high-resolution transmission electron micrograph of a $Co_{70}Fe_{30}$ film on GaAs(110), in the region of a large surface feature, demonstrating that epitaxy is maintained even in the absence of a smooth interface. Hindmarch *et al.* have also demonstrated deposition of amorphous CoFeB films onto GaAs(001)[56]. One significant advantage of sputter deposition over MBE growth is the ability to easily apply a magnetic field to the structure during film deposition in order to 'set' a further magnetic anisotropy: in MBE the electron-beam surface analysis tools typically employed to study the surface structure during growth are intrinsically incompatible with such a magnetic 'forming' field. Conversely, in sputter deposition, the lack of these surface analysis tools results in reduced information regarding the semiconductor surface reconstruction prior to ferromagnet film growth.

Kardasz *et al.*[80] have performed a comparative study of Fe deposited onto GaAs(001) by thermal evaporation and pulsed-laser deposition (PLD). By using 2 ML thick ^{57}Fe marker-layers and performing conversion electron Mössbauer spectroscopy, they demonstrated that the highly-energetic PLD growth causes significant interdiffusion of Fe into GaAs, with the effect of reducing the interfacial uniaxial magnetic anisotropy by roughly a factor of four in comparison to films deposited by thermal evaporation: highlighting the importance of creating an abrupt, clean ferromagnet/semiconductor interface.

In MBE growth it was, until fairly recently, common for ferromagnetic contacts to semiconductors to be grown at slightly elevated temperatures, usually in the range 50–300 °C. However, low-temperature MBE growth of Fe on GaAs(001) has more recently been used in an attempt to enhance the interface cleanliness by Lee *et al.*[88]. They found that by reducing the GaAs substrate temperature to around 130 K they could suppress both out-diffusion of As and Ga from the substrate, and interfacial intermixing, during Fe film growth. Lee *et al.*[81] also show that similarly low-temperature deposited ultra-thin (2.1-2.8 ML) Fe films exhibited ferromagnetism with a perpendicular magnetic anisotropy. It is now far more common for low-temperature (room-temperature and below) MBE-growth to be used for ferromagnet/semiconductor contact deposition.

Another route which has been suggested for providing enhanced ferromagnet/semiconductor interface cleanliness is to use post-growth thermal processing: care must be taken in choosing suitable thermal anneal conditions due to the chemical reactivity and tendency for intermixing between Fe and GaAs. As the cleanliness of the ferromagnet/semiconductor interface is not only of critical importance for the interfacial uniaxial magnetic anisotropy[80,87], but also for spin-coherent electron transport across the ferromagnet/semiconductor interface[89], in recent years significant research effort has been directed toward determining the structure and properties of the buried interface in these systems, and the influence of thermal treatments.

4.2. *Characterization of the buried interface*

In the earlier literature on ferromagnet/semiconductor interface magnetism, significant effort has been expended on investigating the dependence of the growth of thin Fe films, and their inherent magnetic anisotropies, when deposited onto GaAs(001) surfaces which have undergone a range of treatments in order to prepare different surface reconstructions (see reference 5). We recall that, despite surface preparations which result in either As- or Ga-rich reconstructions, the consensus reached was that the surface reconstruction of the III-V semiconductor prior to ferromagnet film growth has little, if any, influence of the resultant magnetic anisotropy in the ferromagnetic film[64,70]: despite having significant influence on the growth of the ferromagnetic film. It is perhaps not so outrageous a supposition, then, to suggest that the structure of the buried Fe/GaAs(001) interface may be of far greater importance than the initial GaAs(001) surface prior to ferromagnet film deposition in determining the physical properties of the ferromagnetic overlayer.

4.2.1. *Atomic arrangement at the ferromagnet/semiconductor interface*

One must consider that the deposition of the ferromagnetic film also has an influence on the underlying semiconductor surface: promoting atomic outdiffusion primarily of As, but also Ga to a lesser extent. From a theoretical point of view, Erwin *et al.* suggested that Fe adsorption causes the characteristic As-dimers of the reconstructed GaAs(001) surface to become unstable[90]. With this in mind, density functional theory calculations, carried out by Demchenko and Liu, assuming an interface structure based on the GaAs(001)-(1×1) reconstruction, suggest that, due to the preference for Fe-As over Fe-Ga interfacial bonding, As-terminated Fe/GaAs(001) favours an atomically abrupt interface whilst the Ga-terminated structure favours an intermixed interface region over several atomic planes[91]. Driven by these theoretical predictions, efforts to unambiguously determine the detailed atomic structure of the buried Fe/GaAs(001) interface experimentally have begun.

From a combination of x-ray photoelectron spectroscopy, reflection high-energy electron diffraction, and photoelectron diffraction, Schieffer *et al.* have suggest the formation of a bcc-Fe-based substitutional alloy during the first 4 ML of Fe growth on the GaAs(001)-(4×2) surface, followed by pure-Fe growth thereafter[92]. Whilst spectroscopy and scattering techniques prove useful, it is clear that microscopic imaging techniques are preferable for precise determination of the interface structure.

Cross-sectional transmission electron microscopy, using both the high-resolution (HRTEM) and high-angle annular-dark-field (HAADF) modes of operation, has been used to measure the interface structure in both the Fe/AlGaAs(001)[93] and Fe/GaAs(001) systems[72]. For Fe/AlGaAs(001), Zega *et al.* found that a post-growth anneal for 10 minutes at 200 °C both reduced the intermixed interface width and increased the injected spin-polarization. Using HAADF (Z-contrast) imaging, a technique which is chemically sensitive at high spatial resolution, a model interface structure consisting of As-terminated AlGaAs-(1×1) with a single intermixed ML of Fe and As at the interface was proposed[93]. However, this study consisted only of cross-sectional images of the interface viewed along the in-plane AlGaAs$[1\bar{1}0]$ direction: Lebeau *et al.* extended this study by taking HAADF images along both the GaAs$[1\bar{1}0]$ and [110] directions in order to unambiguously determine the interface structure in a Fe/GaAs(001) contact, after annealing for 1 hour at 200 °C. They found a subtly different, novel interface structure, shown in figure 4, consisting of As-terminated GaAs(001)-(1×1) and a partially-occupied, non-intermixed, interfacial Fe layer, terminating at the interface-plane.

Further studies on the influence of thermal anneal processing on the structure of the Fe/GaAs(001) interface by Schultz *et al.* have shown that temperatures in the region of 400-450 °C promote the diffusion of both Fe into GaAs (forming Fe_2As clusters) and Ga into Fe (forming an additional Fe_3Ga interface layer). The formation of these two distinct stable binary phases due to interdiffusion occurs preferentially to the anticipated stable $Fe_3Ga_{2-x}As_x$ ternary alloy phase due to Fe being more weakly diffusive that Ga or As in this system[94]. Schultz *et al.* have also demonstrated the influence of such an interfacial Fe_3Ga alloy, in this case formed during elevated-temperature growth, on the spin-injection from Fe into GaAs; showing a reversal in the sign of the injected spin-polarized current from majority- to minority-spin at a growth temperature of 175 °C. Further post-deposition thermal treatment, for 1 hour at 250 °C results in the sign of the injected spin-polarization reverting to majority-spin[89], demonstrative of atomic rearrangement at the Fe/GaAs(001) interface.

The influence of thermal annealing on the interfacial magnetic anisotropy has been studied by Bianco *et al.*[33], who demonstrated an enhancement in the interfacial uniaxial magnetic anisotropy in $Co_{69}Fe_{31}$/GaAs(001) by a factor of three after annealing at 200 °C for 10 mins. They show that the anneal treatment does not result in a significant change in strain, and attribute the enhanced uniaxial magnetic anisotropy to improvements in interfacial bonding, i.e. atomic rearrangement, brought about by the thermal treatment. One may anticipate different interfacial alloys to form due to interdiffusion at the CoFe/GaAs(001) interface, due to the increased diffusivity of Co compared to Fe in GaAs. Given that the magnetic anisotropy and spin-injection efficiency depend critically on the atomic structure at the interface, it seems pertinent also to consider interface magnetism in these structures.

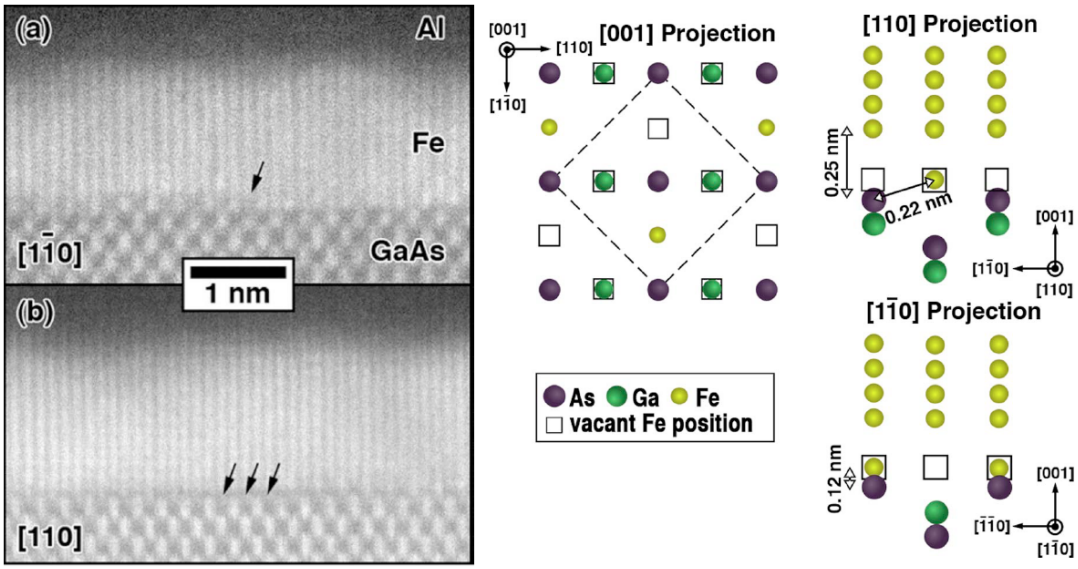

Fig. 4. Left: high-angle annular-dark-field images of epitaxial Fe/GaAs(001), viewed along (a) GaAs[1$\bar{1}$0], and (b) GaAs[110] directions. Right: model structure for the Fe/GaAs(001) interface, showing a partially-occupied, non-intermixed, Fe interface layer. (Reprinted with permission from LeBeau *et al.*[72]. Copyright (2008), American Institute of Physics.)

4.2.2. *Ferromagnet/semiconductor interface magnetism*

Early studies of Fe on GaAs(001) suggested that, for ultra-thin films, the onset of room-temperature ferromagnetism occurs at higher Fe film thickness than may be anticipated from Fe growth on metals. For example, Kneedler *et al.* find ferromagnetism only for Fe films thicker that 6 ML (grown on GaAs(001)-(2 × 4) and GaAs(001)-c(4 × 4))[64], whilst Xu *et al.* showed that their Fe films (grown on GaAs(001)-(4 × 6)) were non-magnetic below 3.5 ML, consisted of superparamagnetic islands between 3.5 and 5 ML, and were ferromagnetic above 5 ML[95]. Such a magnetically 'dead' layer at the interface is quite apparently detrimental for spin-injection applications. Indeed, for many years, suggestions were made that the interfacial magnetic dead-layer found in Fe/GaAs(001) structures may not, in-fact, be an intrinsic feature of the interface between Fe and GaAs(001).

The first demonstration that it is possible for an Fe film to possess its full magnetic moment right up to the interface with GaAs(001) was provided by Claydon *et al.*[96] using x-ray magnetic circular dichroism (XMCD) spectroscopy[97]. They deposited thin Fe films (0.25 – 18 ML) where the thinnest films were buried below Co in order to remain ferromagnetic. Utilizing the element specificity of XMCD, the orbital- and spin-components of the Fe magnetic moments were extracted, demonstrating a bulk-like value for the Fe spin magnetic moment and a large enhancement in the orbital magnetic moment due to the reduced symmetry at the interface. (Bulk-like Fe magnetic moments at the Fe/GaAs(001) interface were later theoretically predicted by calculations of Demchenko and Liu[91], and Tobin *et al.* have used spin-resolved photoelectron spectroscopy to also reveal bulk-like magnetism at the Fe/GaAs(001) interface, despite significant intermixing[74].)

A similar experimental method, again employing the element-specificity of XMCD, has been used by Giovanelli *et al.*[78,79], who have studied the spin and orbital magnetic-moments in a 0.5 ML Co marker layer, as its position is moved through a 6 ML Fe film on GaAs(001). They find that the spin magnetic moment of the Co marker layer is highest in the center of the film, and drops at both the GaAs and vacuum interfaces. A large enhancement in the orbital magnetic moment is again found close to the interface with GaAs(001), as was found by Claydon *et al.*[96]. As the films employed by both groups were deposited onto the GaAs(001)-(4×6) surface, the reason for the discrepancy in behaviour of the interfacial spin magnetic moment is unknown, and may again be related to a different behaviour of Co and Fe atomic species at the interface with GaAs(001).

Whilst photoelectron spectroscopies are pow-

erful techniques, e.g., for determining element-specific magnetic properties, they are less suitable for obtaining depth-selective magnetic information. In order to obtain such information, scattering techniques are commonly employed. The applicability of soft-x-ray resonant magnetic (exchange) scattering (XRMS) to study interface magnetism in ferromagnet/semiconductor contacts has been demonstrated, for example, by Hindmarch *et al.*[87]. They used off-specular XRMS to record element-specific rocking curves, and compared the magnetic disorder with the structural disorder: showing that, even under a saturating magnetic field, interfacial magnetic disorder was present in a $Co_{70}Fe_{30}/Al_{10}Ga_{90}As(001)$ contact. The presence of interfacial magnetic disorder in these structures was correlated with a reduction in the strength of the interfacial uniaxial magnetic anisotropy. Resonant x-ray techniques are useful due to their element specificity. However, quantitative analysis of XRMS is difficult, due in no small part to the indirect nature of the spin-photon interaction upon which it relies. The far more direct interaction of the *neutron* with the local magnetization makes polarized neutron reflectivity (PNR)[98] an attractive technique from which to obtain quantitative, depth-selective information on the magnetization of thin-film structures[99].

Magnetic depth profiling studies of epitaxial CoFe/GaAs(001) structures has been reported by Park *et al.* using PNR[100]. They found that, for an epitaxial CoFe[20 nm] film grown on the GaAs(001)-(2×4) reconstructed surface at 95 °C, the resultant 'magnetic thickness' was reduced from the structural thickness of the CoFe film by around 6 Å; indicative again of a magnetic dead-layer at the CoFe/GaAs(001) interface — the dead-layer thickness in CoFe is somewhat thinner than those typically found in Fe on GaAs(001), again suggesting a different behaviour of Co and Fe elemental species at the GaAs(001) interface. Park *et al.* have further used the PNR technique to investigate the influences of both growth- and anneal-temperatures in epitaxial CoFe, again deposited onto GaAs(001)-(2×4)[101]. They found that reducing the temperature of the CoFe growth resulted in improved interface sharpness and, for CoFe growth at −15 °C, resulted in an interface free of any degraded magnetically dead layer. They also found that, for samples grown at any temperature (within the studied range of −15–175 °C), anneal processing at 250 °C for 1 hour resulted in an 11 Å thick interfacial dead-layer forming: showing that annealing at elevated temperatures and long times can be highly detrimental to the interfacial magnetic properties of the contact.

In an interesting twist on the discussion of the usual quasistatic magnetization reversal, Zhao *et al.* have demonstrated that the magnetization in the interfacial Fe layer appears decoupled from the bulk of the film: it appears to reverse as if possessing only uniaxial magnetic anisotropy, whilst the remainder of the film appears to reverse as if acted on by a admixture of uniaxial and cubic anisotropies[45]. They used a combination of (bulk-sensitive) magneto-optical Kerr effect and (interface-sensitive) magnetization-induced second-harmonic generation magnetometry techniques on Fe/AlGaAs(001) structures to show that, despite being coupled together via the strong exchange field in Fe, in-plane angles in the range 40°– 85° may open between interfacial and bulk magnetic moments. Using time-resolved variants of these techniques, Zhao *et al.* have further determined the angular-dependence of the damping parameter in Fe/AlGaAs(001) from time-resolved Kerr effect magnetometry[102], and investigated the precessional dynamics of Fe moments at the interface with AlGaAs(001) using the time-resolved second-harmonic generation[103]. These surprising and unanticipated demonstrations that the interfacial and bulk magnetization, and their respective dynamical behaviours, are decoupled to such an extent, clearly shows that there is much still to be learned about interface magnetism in ferromagnet/semiconductor hybrid structures.

5. Tailoring the free-energy density

In order to gain further insight into the magnetic anisotropy arising at the ferromagnet/semiconductor interface, it is instructive to find ways in which one may controllably modify the angular-dependence of the free-energy density, equation 3, in a ferromagnetic thin-film on GaAs(001). The full expression for the free-energy density ε for a (Co-rich) CoFe film consisting of terms relating to the cubic magnetocrystalline anisotropy, magnetoelastic anisotropy, interfacial-induced uniaxial magnetic anisotropy, volume magnetization-induced uniaxial magnetic

anisotropy[104], and Zeeman energy, may be written

$$\varepsilon(\phi) \sim -\frac{K_1^{\text{eff}}}{4}\sin^2(2\phi) - \frac{B_2\epsilon}{2}\sin^2(2\phi) + \frac{K_U^{\text{int}}}{t}\sin^2(\phi) + K_U^{\text{vol}}\sin^2(\beta) - HM_S\cos(\phi-\alpha), \quad (8)$$

where α is the angle between the applied magnetic field and the GaAs[110] during measurement, and β is the angle between the applied (saturating) magnetic field and the GaAs[110] during film deposition.

Equation 8 contains numerous terms of differing symmetry and origin, making quantitative analysis difficult: a problem which has previously hindered advance in unravelling the details of the ferromagnet/semiconductor interface anisotropy. However, by judicious choice of ferromagnetic thin-film material, one is able to significantly simplify equation 8 by 'removing' various terms in the free-energy density; thereby making the physical origins of the various magnetic anisotropy contributions more easily experimentally accessible.

5.1. *Removal of the magnetoelastic anisotropy term*

As discussed in section 3.1, one mechanism which has been extensively suggested as underpinning the uniaxial interfacial magnetic anisotropy is epitaxial strain in the ferromagnetic film. Both in experimental work reported by Thomas *et al.*[41] and by Bianco *et al.*[33], and in previous theoretical work presented by Sjöstedt *et al.*[71], evidence to the contrary has been provided: uniaxial magnetic anisotropy arises in the absence of epitaxial strain.

We would thus like to find a ferromagnetic metal where the lattice mismatch with GaAs, and hence epitaxial strain, is negligible. Although it is common in the literature to disregard the magnetoelastic term, for Fe the lattice-constant of $d = 2.86$ Å results in epitaxial strain of around 1.4 % when deposited on GaAs (table 2). Epitaxial $Co_{70}Fe_{30}$ films have negligible lattice mismatch with GaAs: for $Co_{70}Fe_{30}$ $d \approx 2.835$ Å[29], hence when using $Co_{70}Fe_{30}$, the magnetoelastic term is indeed negligible. For this CoFe composition the second-order cubic anisotropy constant K_2 is negligible and the omission of this term also is justified[28].

5.1.1. *Interfacial magnetic anisotropy in epitaxial films*

One obvious question to ask is whether we see an effect by changing the III-V semiconductor *material*, keeping all other factors constant. In order that the magnetoelastic term in equation 8 remain negligible, we have compared $Co_{70}Fe_{30}$ films deposited on GaAs(001) and $Al_{30}Ga_{70}As$(001) surfaces. In the absence of an applied magnetic field during film deposition, equation 8 reduces to equation 4, the expression for the free-energy density which is commonly applied to epitaxial CoFe on GaAs(001),

$$\varepsilon(\phi) \sim -\frac{K_1^{\text{eff}}}{4}\sin^2(2\phi) + \frac{K_U^{\text{int}}}{t}\sin^2(\phi) - HM_S\cos(\phi-\alpha).$$

Figure 5 shows magneto-optical Kerr-effect hysteresis loops along the uniaxial hard-axis for $Co_{70}Fe_{30}$ films on GaAs(001) (a) and $Al_{30}Ga_{70}As$(001) (b): we are clearly able to observe interfacial uniaxial magnetic anisotropy in epitaxial sputtered $Co_{70}Fe_{30}$ films. The effective anisotropy constants are $K_1^{\text{eff}} \approx -2.8 \times 10^4$ J/m^3 and $K_U^{\text{eff}} = K_U^{\text{int}}/t \approx 1.5 \times 10^4$ J/m^3 for $Co_{70}Fe_{30}$ on both GaAs(001) and $Al_{30}Ga_{70}As$(001).

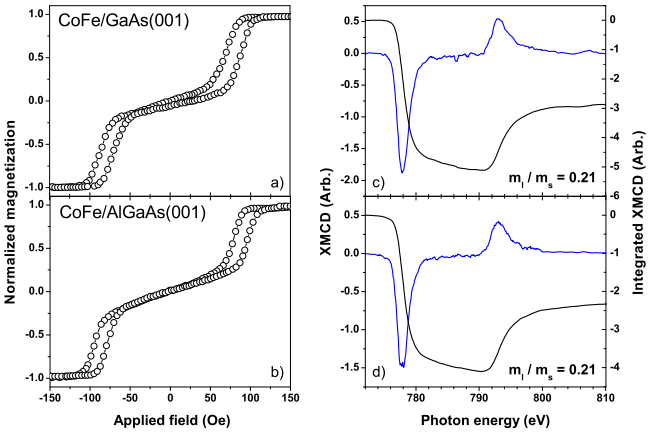

Fig. 5. MOKE hysteresis loops along the uniaxial hard axis for $Co_{70}Fe_{30}$[3.5 nm] on (a) GaAs and (b) $Al_{30}Ga_{70}As$, and Co-edge XMCD spectra for $Co_{70}Fe_{30}$ on (c) GaAs and (d) $Al_{30}Ga_{70}As$. Similar magnetic anisotropies are obtained for both films and the orbital:spin magnetic moment ratio extracted from sum-rule analysis of the XMCD spectra are identical.

XMCD spectra around the Co L_{II} and L_{III} absorption edges are also shown in figure 5 for films on GaAs (c) and $Al_{30}Ga_{70}As$ (d) with magnetization along the uniaxial easy-axis. For both films the ratio of orbital to spin magnetic moments are extracted using sum-rule analysis[105], and are found to be $m_l/m_s = 0.21$ for Co, and $m_l/m_s = 0.11$ for Fe (not shown), apparently independent of the underlying semiconductor material. For a ferromagnet with *only* uniaxial anisotropy, m_l/m_s measured

along the uniaxial easy axis should be proportional to the degree of anisotropy in m_l, and hence to the effective uniaxial magnetic anisotropy[25,27]. However, in this case there is also a volume cubic magnetocrystalline anisotropy with similar strength to the interface induced uniaxial magnetic anisotropy: the measured anisotropy in m_l is due predominantly to the magnetocrystalline anisotropy, owing to the short penetration-depth of electron-yield XMCD.

One could, at this point, conclude that the underlying compound semiconductor material plays no rôle in the uniaxial magnetic anisotropy in the absence of epitaxial strain. Rather, we suggest that it is difficult to accurately determine the effect of the substrate material on the uniaxial magnetic anisotropy in epitaxial films due to the interplay with the cubic magnetocrystalline anisotropy: as the m_l/m_s are biased toward the volume rather than interfacial moments, one may again obtain little information on the origin of the *interfacial* uniaxial magnetic anisotropy from XMCD on epitaxial ferromagnetic films on GaAs(001), and a subtly different approach is necessary.

5.1.2. *Modification of the volume uniaxial anisotropy term*

Before continuing to further simplify the expression for the free-energy density, we first consider the effects of reintroducing the volume magnetization-induced uniaxial magnetic anisotropy term to equation 4, giving

$$\begin{aligned}\varepsilon(\phi) \;&\sim -\tfrac{K_{\mathrm{l}}^{\mathrm{eff}}}{4}\sin^2(2\phi) + \tfrac{K_{\mathrm{U}}^{\mathrm{int}}}{t}\sin^2(\phi) \\ &\quad + K_{\mathrm{U}}^{\mathrm{vol}}\sin^2(\beta) - HM_{\mathrm{S}}\cos(\phi-\alpha)\,. \qquad (9)\end{aligned}$$

It then appears a trivial matter to separate the contributions from magnetization- and interface-induced uniaxial magnetic anisotropies from either the thickness, t, or angular, ϕ and/or α, dependence.

Magneto-optical Kerr-effect hysteresis loops for a series of thin $Co_{70}Fe_{30}$ films on GaAs(001) are shown in figure 6a), which have been sputter-deposited in either zero applied magnetic field, or with a saturating magnetic field, H_{Dep}, applied along either the easy- or hard-axis of the interfacial uniaxial magnetic anisotropy ([110] or [1$\bar{1}$0]): the effective magnetic anisotropy constants are given in table 3. It is found that applying a magnetic field along the [110] direction during film growth has a negligible effect on the magnetic anisotropy, whilst applying a magnetic field along [1$\bar{1}$0], the *hard-axis* of the interface-induced anisotropy, results in an *increase* in the effective uniaxial magnetic anisotropy.

The reason for this may be revealed from XMCD spectroscopy: figures 6b)-d) show XMCD spectra around the Co and Fe L_{II} and L_{III} absorption edges for these films. Significant differences in the ratio of orbital-to-spin magnetic moments between films deposited with and without an applied magnetic field are observed. Applying the deposition field along the interfacial uniaxial easy-axis produces an increase in the component of the ratio of the atomic species resolved orbital and spin magnetic moments, m_l/m_s, directed along the uniaxial easy axis of magnetization, whilst applying the deposition field along the uniaxial hard-axis causes a decrease, as summarized in table 3. The ratio m_l/m_s along the easy-axis may be taken as representative of the degree of anisotropy in the orbital magnetic moment, and hence as a measure of the magnetic anisotropy itself[27]. The spin-orbit contribution to the uniaxial magnetic anisotropy is $\Delta E_{\mathrm{SO}} \propto -\boldsymbol{m}_l \cdot \boldsymbol{m}_s \sim -m_l$[34]; hence the deposition field changes the maximal projection of the atomic orbital magnetic moments onto the easy-axis, which corresponds to a deposition-field-induced shift in the free-energy landscape via a modification of the contribution of the spin-orbit interaction to the total energy.

5.2. *Removal of the magnetocrystalline anisotropy term*

It is clear that the spin-orbit interaction plays a pivotal rôle in determining the magnetic anisotropy in epitaxial ferromagnetic films: in a crystalline ferromagnetic film the orbital moment contributes both to the uniaxial *and* cubic magnetocrystalline anisotropies. Due to this fact, the origin of the interface-induced uniaxial magnetic anisotropy is partially obscured — in order to disentangle these influences, crystalline ferromagnets must be abandoned.

Using an amorphous ferromagnet, i.e. one having no long-range crystal symmetry, it is possible to isolate the interfacial magnetic anisotropy, by entirely removing the magnetocrystalline anisotropy contribution. The expression for the free-energy density then reduces to the trivial form

$$\varepsilon(\phi) \sim \frac{K_{\mathrm{U}}^{\mathrm{int}}}{t}\sin^2(\phi) - HM_{\mathrm{S}}\cos(\phi-\alpha): \qquad (10)$$

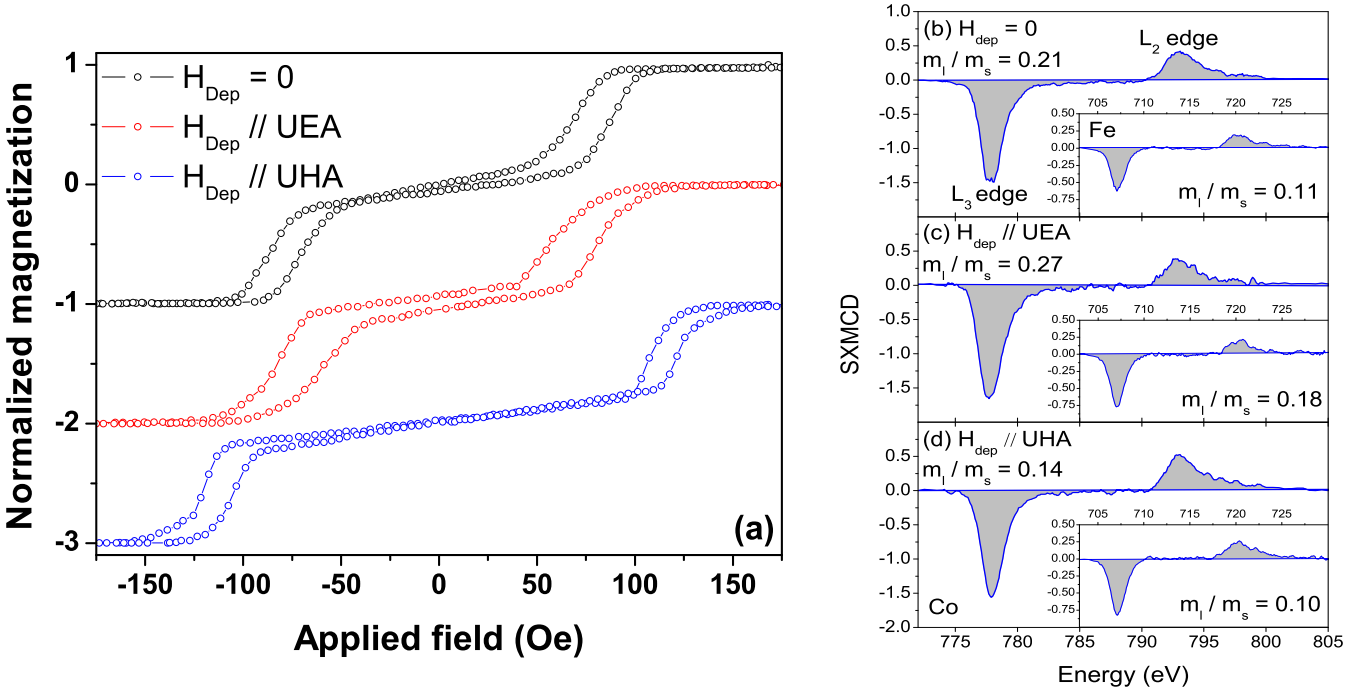

Fig. 6. (Color online) Room temperature magnetic hysteresis loops (a) for epitaxial $Co_{70}Fe_{30}$[3.5 nm] films on GaAs(001) deposited with no applied field and magnetic fields parallel to the interfacial uniaxial easy- and hard-axes. XMCD spectra around the Co (main) and Fe (inset) L_{II} and L_{III} edges for (b) zero magnetic field, (c) magnetic field applied along the uniaxial easy axis, and (d) magnetic field applied along the uniaxial hard axis. The orbital-to-spin magnetic-moment ratios m_l/m_s extracted from sum-rule analysis are indicated. (After Hindmarch *et al.*[34].)

Table 3. Summary of the effective uniaxial and cubic magnetic anisotropy constants (equation 2), and XMCD m_l/m_s ratios along the uniaxial easy-axis, for epitaxial $Co_{70}Fe_{30}$[3.5 nm] films on GaAs(001). (After Hindmarch *et al.*[34].)

	$H_{\rm Dep} = 0$	$H_{\rm Dep}$ // UEA	$H_{\rm Dep}$ // UHA
$K_{\rm U}^{\rm eff}$ ($\times 10^5$ erg/cc)	1.5 ± 0.1	1.4 ± 0.1	2.1 ± 0.1
$K_1^{\rm eff}$ ($\times 10^5$ erg/cc)	-2.8 ± 0.1	-2.8 ± 0.1	-2.2 ± 0.1
$K_1^{\rm eff}/K_{\rm U}^{\rm eff}$	-1.9 ± 0.1	-2.0 ± 0.1	-1.05 ± 0.1
m_l/m_s (Co)	0.21 ± 0.02	0.27 ± 0.02	0.14 ± 0.02
m_l/m_s (Fe)	0.11 ± 0.02	0.18 ± 0.02	0.10 ± 0.02

no cubic magnetocrystalline anisotropy is present, and the origin of the uniaxial magnetic anisotropy should be more easily accessible experimentally[56].

An amorphous ferromagnet may be produced by alloying dilute metalloid into the ferromagnetic metal matrix: addition of ∼20% metalloid (for example, boron) in the ferromagnetic transition metal alloy, CoFe, slightly reduces the Curie temperature and saturation magnetization relative to CoFe, whilst at the same time destroying long-range crystalline order. HRTEM micrographs of $Co_{40}Fe_{40}B_{20}$[3.5 nm] films on GaAs(001) and $Al_{30}Ga_{70}As$(001) surfaces are shown in figure 7: the clear crystallinity of the underlying semiconductor terminates abruptly at the interface with the CoFeB layer, which is amorphous. For films on the GaAs(001) substrate, a surface corrugation is observed when viewed along the $[1\bar{1}0]$ direction, figure 7b), with amplitude Δ and period ξ indicated. A longer period corrugation, $\xi \sim$ 100s nm, is found at the surface of $Al_{30}Ga_{70}As$(001).

5.2.1. *Interfacial magnetic anisotropy in amorphous films*

To demonstrate that the interfacial uniaxial magnetic anisotropy is still present for amorphous ferromagnetic films on III-V(001) surfaces, magneto-optical Kerr-effect hysteresis loops for $Co_{40}Fe_{40}B_{20}$[3.5 nm] films on GaAs(001) and $Al_{30}Ga_{70}As$(001) are shown in figure 8. In this case the films were deposited in an applied magnetic field along the GaAs[$1\bar{1}0$] direction (adding a volume uniaxial magnetic anisotropy term to the free-energy density for each film): the magnetic field during measurement is applied either parallel or perpendicular to the deposition field. Strong uniaxial magnetic anisotropy is observed in both films, and the uniaxial easy-axes are *perpendicular* to the applied deposition field direction: indicating that the uniaxial magnetic anisotropy is not simply of a magnetization-induced origin.

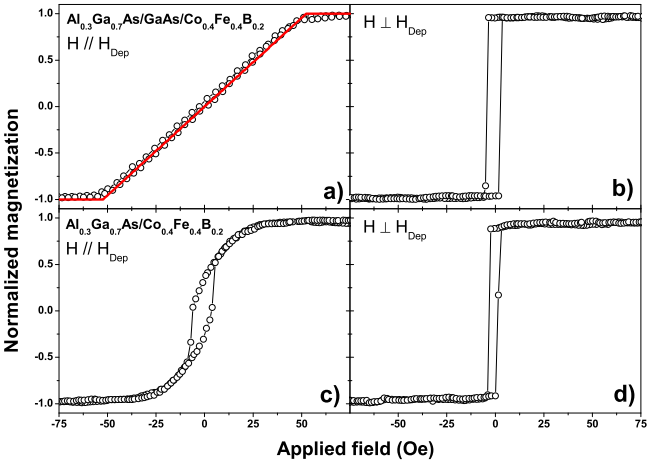

Fig. 8. Hysteresis loops of $Co_{40}Fe_{40}B_{20}$[3.5 nm] films on GaAs(001), a) & b), and $Al_{30}Ga_{70}As$(001), c) & d). The field is applied parallel or perpendicular to the deposition field, as indicated. The solid red line in frame a) is a fit using the Stoner-Wohlfarth model for the free-energy density, based on equation 10. (After Hindmarch *et al.*[56].)

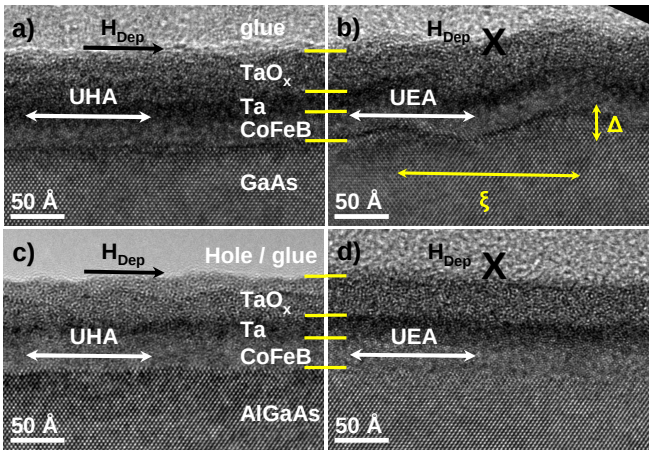

Fig. 7. Cross-sectional HRTEM micrographs of $Co_{40}Fe_{40}B_{20}$/GaAs/$Al_{30}Ga_{70}As$(001), a) & b), and $Co_{40}Fe_{40}B_{20}$/$Al_{30}Ga_{70}As$(001), c) & d), contacts. The growth field direction and uniaxial magnetic anisotropy axes are indicated in each frame. The corrugation period ξ and amplitude Δ are indicated in frame b). (After Hindmarch *et al.*[56].)

$Co_{40}Fe_{40}B_{20}$ films on GaAs(001) exhibit an entirely reversible magnetization reversal by coherent rotation for fields applied along the hard-axis; whereas for $Al_{30}Ga_{70}As$(001), hard-axis reversal takes place partially by domain wall motion. The uniaxial anisotropy field is also reduced for $Al_{30}Ga_{70}As$(001), indicating a stronger uniaxial magnetic anisotropy in structures with GaAs(001). The reason for the difference in reversal-mechanism may be explained due to the surface corrugation: one may calculate a Néel-type domain-wall width[30] of $D \sim 150$ nm for these $Co_{40}Fe_{40}B_{20}$ films: it seems reasonable that the substrate surface corrugation is able to influence domain-walls for $Co_{40}Fe_{40}B_{20}$ on $Al_{30}Ga_{70}As$(001), where $D \sim \xi$. Fortuitously, the orientation of the surface corrugation relative the the easy-axis of the uniaxial magnetic anisotropy allows step-edge anisotropies also to be ruled out as contributory factors in determining the magnetic anisotropy[56]. Indeed, the only mechanism which may plausibly explain both the direction and magnitude of the uniaxial magnetic anisotropy is the interface-interaction between ferromagnetic metals and III-V(001) semiconductors; despite the lack of crystal symmetry in the $Co_{40}Fe_{40}B_{20}$ films.

The important question which must be answered is, what determines the difference in strength of the uniaxial magnetic anisotropy in $Al_{30}Ga_{70}As$ compared to GaAs? It is well known that orbital angular momentum plays a dominant rôle in determining the strength of magnetocrys-

talline anisotropy; applying XMCD spectroscopy to these films allows determination of the orbital- and spin-resolved components of the atomic magnetic moments in both Co and Fe atomic species, demonstrating that the different semiconductor alloy surfaces influence the uniaxial magnetic anisotropy through the orbital component of the atomic magnetic moments.

Interfacial bonding, long thought to be important in determining the interfacial magnetic anisotropy, is found not, in-fact, to be the whole story: no significant difference in interface bonding charge transfer between $Co_{40}Fe_{40}B_{20}$ films on $Al_{30}Ga_{70}As(001)$ and GaAs(001) at either Co or Fe sites, from the integrated absorption spectra[69]. This may be anticipated as the fraction of interfacial As sites is unchanged — whilst interfacial bonding may be important in determining the *directionality*, another factor must be at play in determining the *strength* of the uniaxial magnetic anisotropy.

Table 4. Ratios of the orbital–to-spin magnetic moments for Fe and Co atomic species in amorphous $Co_{40}Fe_{40}B_{20}$[3.5 nm] films on GaAs(001) and $Al_{30}Ga_{70}As(001)$ as measured by XMCD. (After Hindmarch *et al.*[56].)

Species	GaAs	$Al_{30}Ga_{70}As$
Fe	$m_l/m_s = 0.45$	$m_l/m_s = 0.34$
Co	$m_l/m_s = 0.38$	$m_l/m_s = 0.19$

The results of sum-rule analysis of the recorded XMCD spectra for $Co_{40}Fe_{40}B_{20}$ films on GaAs(001) and $Al_{30}Ga_{70}As(001)$ are shown in table 4. In all cases moments are enhanced over those for CoFe alloys (table 3) and elemental metals (for bulk elemental Fe $m_l/m_s = 0.043$, and for Co $m_l/m_s = 0.099$[105]) due the the reduced orbital moment quenching arising from the lack of crystal symmetry in CoFeB. The observed differences between the m_l/m_s ratios for films on GaAs(001) and $Al_{30}Ga_{70}As(001)$ are unrelated to interfacial bonding, and, due to the electronic structure of CoFe(B) alloys, cannot arise due to charge transfer via internal bonding and back-donation interactions[56,106].

Additional enhancement in the atomic orbital moment can occur in systems which exhibit a spin-reorientation transition, where the enhancement is related to a non-local spin-orbit interaction which modifies the anisotropy in the magnetic layer due to the strongly spin-orbit coupled adjacent material, e.g., Co/Au or Co/Pt[107]. The criteria for this enhancement to occur are that there should be strong spin-orbit coupling in the adjacent material, and, strong wavefunction overlap across the interface,i.e., strong interfacial bonding[107]. As discussed previously, the bonding across the ferromagnet/GaAs(001) interface is well-known to be strong, and to be capable of influencing the electronic structure in the ferromagnetic metal[69]: and, as the spin-orbit interaction parameters in Au and Pt are ~ 0.005 eV, compound semiconductors have far stronger valence spin-orbit coupling (Table 2) than these elemental metals.

Comparing the spin-orbit coupling strength in GaAs ($\Delta_0 = 0.34$ eV) and the series of AlGaAs alloys ($0.3 \leq \Delta_0 \leq 0.34$ eV), we see that adding Al to GaAs causes a reduction in the valence spin-orbit coupling. Were the uniaxial magnetic anisotropy in the ferromagnetic overlayer to be related to the non-local spin-orbit interaction, we would anticipate a weaker uniaxial magnetic anisotropy for films on $Al_{30}Ga_{70}As(001)$ than for films on GaAs(001): as is found in these CoFeB films, and also by Zakeri *et al.* for epitaxial Fe/InP(001) (which has $\Delta_0 = 0.11$ eV, table 2). Whilst interfacial-bonding is crucially important, both in determining the *direction* of the uniaxial magnetic anisotropy and in allowing the non-local spin-orbit interaction to couple to the ferromagnetic film, the observed differences in the strength of the uniaxial magnetic anisotropy, figure 8, and species-resolved orbital magnetic moments, table 4, seems to point toward the spin-orbit coupling strength in the semiconductor playing a rôle in producing the interface-induced uniaxial magnetic anisotropy in ferromagnetic films on the (001) surface of III-V compound semiconductors.

In this section we have discussed several means by which the in-plane magnetic anisotropies in ferromagnet-III-V(001) hybrid contacts may be modified, and suggest a possible explanation for the origin of the interfacial uniaxial magnetic anisotropy. Despite these recent advances, there is much work still to be done in fully understanding the intriguing magnetic behavour exhibited by this class of structures.

6. Perspectives

One of the so-called 'grand challenges' in nanomagnetism today is to harness the ability to manipulate the magnetization direction using an electric field. The electric-field strength predicted to be required in order to significantly modify the magnetic anisotropy in Fe monolayer has been calculated to be up to 1 V/Å (10^8 V/cm)[108] — a very strong electric field in comparison to the dielectric breakdown threshold of GaAs. However, Ohta *et al.* used magneto-optical measurements under an AC backgate voltage applied across the Schottky barrier in a thin Fe film on n-GaAs(001) with in-plane magnetization[109], and showed a change in Kerr-ellipticity with application of a comparatively weak electric field: they applied a voltage of 1 V across a Schottky barrier with $n = 5\times10^{17}$ cm^{-3} (depletion width $\sim$ 24 nm), i.e., an electric field of order 0.005 V/Å — comparable to the dielectric breakdown threshold[6]. However, other groups have been unable to verify this result using other magnetometry techniques, suggesting that 'parasitic' electro-optic or piezoelectric effects may play a more significant role than originally suggested in reference 109. A successful method for obtaining voltage-control of a ferromagnet is to indirectly couple the voltage to the magnetization via mechanical strain: applying a voltage to a piezo-stressor attached to the film results in a macroscopic strain of $\sim 10^{-5}$ V^{-1}: significant changes in anisotropy may be achieved with relatively modest voltages[110] using the Villari effect[111]. Recently, Nolting *et al.* have demonstrated that the x-ray magnetic linear dichroism technique may be used to attempt to distinguish spin-orbit and strain effects in Fe/GaAs(001) structures[112].

An area not touched on so-far in this article has been the incorporation of a *ferromagnetic* semiconductor into the hybrid structure, the archetypal example being GaMnAs. The major stumbling-block to application of these materials is the low Curie-temperatures, below room-temperature, which make spintronic devices based on dilute magnetic semiconductors impractical for most applications. However, Maccherozzi *et al.* found that in epitaxial Fe/GaMnAs/GaAs(001) structures, an interfacial proximity effect allows the exchange interaction in the Fe film to stabilize interfacial ferromagnetism in GaMnAs to room temperature. Olejnik *et al.* found that, in a similar structure, the Fe layer causes an exchange-bias effect on the GaMnAs layer when cooled through its Curie temperature: the direction of the exchange-bias is controlled by the direction in which the Fe film is magnetized during cooling[73]. Mark *et al.* deposited $Ni_{80}Fe_{20}$/GaMnAs/GaAs(001) films, and found an absence of exchange coupling across the interface in these materials; in effect producing an abrupt, and tuneable, magnetization gradient at the interface between $Ni_{80}Fe_{20}$ and GaMnAs. These results show great potential for enabling room-temperature operation of spintronic devices based on dilute magnetic semiconductors.

The topic of ferromagnetic metal contacts to compound semiconductors has come a long way since its humble beginnings: in 1983 it would have been impossible to augur the impact and extent of the field as it stands at the present day. Whilst a great deal of progress has been made, there are many aspects of the behaviour of hybrid ferromagnet-semiconductor structures which are not well understood, and many exciting discoveries still to be made — although, of course, one cannot predict the nature and potential impact of these discoveries, even in the short-term.

Acknowledgements

The author wishes to thank the many people who have contributed to the work presented here; including C.H. Marrows, D.A. Arena, B.J. Hickey, C.J. Kinane, M. Henini, A.K. Suszka, K.J. Dempsey, D. Taylor, J. Dvorak, M. MacKenzie, and J.N. Chapman. Interesting and fruitful discussions with B.L Gallagher, A.W. Rushforth, K.W. Edmonds, R.P. Campion, C.T. Foxon, T. Jungwirth, J.A. Haigh, J.S. Claydon, M. Ali, D. Ciudad, and G. Burnell are also gratefully acknowledged, as is financial support under EU Grant No. 214499 NAMASTE.

References

1. J. R. Waldrop and R. W. Grant, Interface chemistry of metal-GaAs Schottky-barrier contacts, *Appl. Phys. Lett.* **34**, 630 (1979).
2. W. Jantz, G. Rupp, R. Smith, W. Wettling and G. Bayreuther, Investigation of single crystal Fe films grown by MBE on GaAs substrates, *IEEE Trans. Mag.* **19**, 1859 (1983).
3. J. J. Krebs, B. T. Jonker and G. A. Prinz, Properties of Fe single-crystal films grown on (100)GaAs by molecular-beam epitaxy, *J. Appl. Phys.* **61**, 2596 (1987).

4. G. A. Prinz, Hybrid ferromagnetic-semiconductor structures, *Science* **250**, 1092 (1990).
5. G. Wastlbauer and J. A. C. Bland, Structural and magnetic properties of ultrathin epitaxial Fe films on GaAs(001) and related semiconductor substrates, *Adv. Phys.* **54**, 137 (2005).
6. S. M. Sze, *Physics of semiconductor devices*, 2nd edn. (J. Wiley and sons, 1981).
7. E. I. Rashba, Theory of electrical spin injection: tunnel contacts as a solution of the conductivity mismatch problem, *Phys. Rev. B* **62**, R16267 (2000).
8. Y. Ohno, D. K. Young, B. Beschoten, F. Matsukura, H. Ohno and D. D. Awschalom, Electrical spin injection in a ferromagnetic semiconductor heterostructure, *Nature* **402**, 790 (1999).
9. B. T. Jonker, Progress toward electrical injection of spin-polarized electrons into semiconductors, *Proc. IEEE* **91**, 727 (2003).
10. S. Datta and B. Das, Electronic analog of the electro-optic modulator, *Appl. Phys. Lett.* **56**, 665 (1990).
11. S. A. Crooker, M. Furis, X. Lou, C. Adelmann, D. L. Smith, C. J. Palmstrøm and P. A. Crowell, Imaging spin transport in lateral ferromagnet/semiconductor structures, *Science* **309**, 2191 (2005).
12. P. Kotissek, M. Bailleul, M. Sperl, A. Spitzer, D. Schuh, W. Wegscheider, C. H. Back and G. Bayreuther, Cross-sectional imaging of spin injection into a semiconductor, *Nature Phys.* **3**, 872 (2007).
13. X. Lou, C. Adelmann, M. Furis, S. A. Crooker, C. J. Palmstrøm and P. A. Crowell, Electrical detection of spin accumulation at a ferromagnet-semiconductor interface, *Phys. Rev. Lett.* **96**, 176603 (2006).
14. X. Lou, C. Adelmann, S. A. Crooker, E. S. Garlid, J. Zhang, K. S. M. Reddy, S. D. Flexner, C. J. Palmstrom and P. A. Crowell, Electrical detection of spin transport in lateral ferromagnet-semiconductor devices, *Nature Phys.* **3**, 197 (2007).
15. E. S. Garlid, Q. O. Hu, M. K. Chan, C. J. Palmstrøm and P. A. Crowell, Electrical measurement of the direct spin Hall effect in $Fe/In_xGa_{1-x}As$ heterostructures, *Phys. Rev. Lett.* **105**, 156602 (2010).
16. X. G. Zhang and W. H. Butler, Large magnetoresistance in bcc Co/MgO/Co and FeCo/MgO/FeCo tunnel junctions, *Phys. Rev. B* **70**, 172407 (2004).
17. J. Moser, M. Zenger, C. Gerl, D. Schuh, R. Meier, P. Chen, G. Bayreuther, W. Wegscheider, D. Weiss, C.-H. Lai, R.-T. Huang, M. Kosuth and H. Ebert, Bias dependent inversion of tunneling magnetoresistance in Fe/GaAs/Fe tunnel junctions, *Appl. Phys. Lett.* **89**, 162106 (2006).
18. G. Autès, J. Mathon and A. Umerski, Theory of tunneling magnetoresistance of Fe/GaAs/Fe(001) junctions, *Phys. Rev. B* **82**, 115212 (2010).
19. X. Jiang, R. Wang, S. van Dijken, R. Shelby, R. Macfarlane, G. S. Solomon, J. Harris and S. S. P. Parkin, Optical detection of hot-electron spin injection into GaAs from a magnetic tunnel transistor source, *Physical Review Letters* **90**, 256603 (2003).
20. S. S. P. Parkin, C. Kaiser, A. Panchula, P. M. Rice, B. Hughes, M. Samant and S. H. Yang, Giant tunnelling magnetoresistance at room temperature with MgO (100) tunnel barriers, *Nature Mat.* **3**, 862 (2004).
21. S. Yuasa, T. Nagahama, A. Fukushima, Y. Suzuki and K. Ando, Giant room-temperature magnetoresistance in single-crystal Fe/MgO/Fe magnetic tunnel junctions, *Nature Mat.* **3**, 868 (2004).
22. G. Autès, J. Mathon and A. Umerski, Strong enhancement of the tunneling magnetoresistance by electron filtering in an Fe/Mgo/Fe/GaAs(001) junction, *Phys. Rev. Lett.* **104**, 217202 (2010).
23. T. Nagahama, H. Saito and S. Yuasa, Hot electron transport in magnetic tunnel transistors with an epitaxial MgO tunnel barrier, *Appl. Phys. Lett.* **96**, 112509 (2010).
24. P. Weiss, Magnetization of crystalline Magnetite, *J. Phys.* **5**, 453 (1896).
25. H. A. Dürr, G. Y. Guo, G. van der Laan, J. Lee, G. Lauhoff and J. A. C. Bland, Element-specific magnetic anisotropy determined by transverse magnetic circular X-ray dichroism, *Science* **277**, 213–215 (1997).
26. S. Chikazumi, *Physics of ferromagnetism* (Oxford University Press, 1997).
27. P. Bruno, Tight-binding approach to the orbital magnetic moment and magnetocrystalline anisotropy of transition-metal monolayers, *Phys. Rev. B* **39**, 865 (1989).
28. R. M. Bozorth, *Ferromagnetism* (Van Nostrand, 1951).
29. W. Ellis and E. Greiner, Equilibrium relations in the solid state of the iron-cobalt system, *Trans. Am. Soc. Met.* **29**, 415 (1941).
30. S. Blundell, *Magnetism in condensed matter* (Oxford University Press, 2001).
31. M. Dumm, B. Uhl, M. Zolfl, W. Kipferl and G. Bayreuther, Volume and interface magnetic anisotropy of $Fe_{1-x}Co_x$ thin films on GaAs(001), *J. Appl. Phys.* **91**, 8763 (2002).
32. M. Dumm, M. Zolfl, R. Moosbuhler, M. Brockmann, T. Schmidt and G. Bayreuther, Magnetism of ultrathin FeCo (001) films on GaAs(001), *J. Appl. Phys.* **87**, 5457 (2000).
33. F. Bianco, P. Bouchon, M. Sousa, G. Salis and S. F. Alvarado, Enhanced uniaxial magnetic anisotropy in $Fe_{31}]Co_{69}$ thin films on GaAs(001), *J. Appl. Phys.* **104**, 083901 (2008).

34. A. T. Hindmarch, D. A. Arena, K. J. Dempsey, M. Henini and C. H. Marrows, Influence of deposition field on the magnetic anisotropy in epitaxial $Co_{70}Fe_{30}$ films on GaAs(001), *Phys. Rev. B* **81**, 100407 (2010).
35. S. J. Blundell, M. Gester, J. A. C. Bland, C. Daboo, E. Gu, M. J. Baird and A. J. R. Ives, Structure induced magnetic anisotropy behavior in Co/GaAs(001) films, *J. Appl. Phys.* **73**, 5948 (1993).
36. Y. Z. Wu, H. F. Ding, C. Jing, D. Wu, G. L. Liu, V. Gordon, G. S. Dong, X. F. Jin, S. Zhu and K. Sun, In-plane magnetic anisotropy of bcc Co on GaAs(001), *Phys. Rev. B* **57**, 11935 (1998).
37. C. S. Tian, D. Qian, D. Wu, R. H. He, Y. Z. Wu, W. X. Tang, L. F. Yin, Y. S. Shi, G. S. Dong, X. F. Jin, X. M. Jiang, F. Q. Liu, H. J. Qian, K. Sun, L. M. Wang, G. Rossi, Z. Q. Qiu and J. Shi, Body-centered-cubic Ni and its magnetic properties, *Phys. Rev. Lett.* **94**, 137210 (2005).
38. L. F. Yin, D. H. Wei, N. Lei, L. H. Zhou, C. S. Tian, G. S. Dong, X. F. Jin, L. P. Guo, Q. J. Jia and R. Q. Wu, Magnetocrystalline anisotropy in permalloy revisited, *Phys. Rev. Lett.* **97**, 067203 (2006).
39. G. Bayreuther, M. Dumm, B. Uhl, R. Meier and W. Kipferl, Magnetocrystalline volume and interface anisotropies in epitaxial films: universal relation and Néel's model, *J. Appl. Phys.* **93**, 8230 (2003).
40. E. C. Stoner and E. P. Wohlfarth, A mechanism of magnetic hysteresis in heterogeneous alloys, *Trans. Roy. Soc.* **240**, 599 (1948).
41. O. Thomas, Q. Shen, P. Schieffer, N. Tournerie and B. Lepine, Interplay between anisotropic strain relaxation and uniaxial interface magnetic anisotropy in epitaxial Fe films on (001) GaAs, *Phys. Rev. Lett* **90**, 017205 (2003).
42. J. S. Claydon, D. X. Niu, Y. B. Xu, N. D. Telling, I. W. Kirkman and G. van der Laan, Spin and orbital moments of ultra-thin Fe films on various semiconductor surfaces, *IEEE Trans. Mag.* **41**, 3325 (2005).
43. K. Zakeri, T. Kebe, J. Lindner and M. Farle, Magnetic anisotropy of Fe/GaAs(001) ultrathin films investigated by in situ ferromagnetic resonance, *J. Magn. Magn. Mater.* **299**, L1 (2006).
44. N. A. Morley, M. R. J. Gibbs, E. Ahmad, I. G. Will and Y. B. Xu, Comparison between the in-plane anisotropies and magnetostriction constants of thin epitaxial Fe films grown on GaAs and $Ga_{0.8}In_{0.2}As$ substrates, with Cr overlayers, *J. Appl. Phys.* **99**, 08N508 (2006).
45. H. B. Zhao, D. Talbayev, G. Lupke, A. T. Hanbicki, C. H. Li, M. J. van't Erve, G. Kioseoglou and B. T. Jonker, Interface magnetization reversal and anisotropy in Fe/AlGaAs(001), *Phys. Rev. Lett* **95**, 137202 (2005).
46. B. Lépine, C. Lallaizon, S. Ababou, A. Guivarc'h, S. Députier, A. Filipe, F. Nguyen Van Dau, A. Schuhl, F. Abel and C. Cohen, Fe/GaAs(001) and Fe/GaSb(001) heterostructures: epitaxial growth and magnetic properties, *J. Crystal Growth* **201-202**, 702 (1999).
47. F. Richomme, A. Fnidiki and J. P. Eymery, Magnetic study of epitaxial Fe/InGaAs/InP(100) deposited by ion-beam sputtering, *J. Appl. Phys.* **97**, 123902 (2005).
48. N. Tournerie, P. Schieffer, B. Lepine, C. Lallaizon and G. Jezequel, Structural and magnetic anisotropy properties in epitaxial Fe films on $Al_{0.48}In_{0.52}As(001)$, *IEEE Trans. Mag.* **41**, 3322 (2005).
49. K. Zakeri, J. Lindner and M. Farle, Thickness-dependent reorientation of the magnetization of Fe monolayers on InP(001), *Europhys. Lett.* **83**, 17006 (2008).
50. Y. B. Xu, D. J. Freeland, M. Tselepi and J. A. C. Bland, Anisotropic lattice relaxation and uniaxial magnetic anisotropy in Fe/InAs(100)-4 × 2, *Phys. Rev. B* **62**, 1167 (2000).
51. J. J. Krebs, B. T. Jonker and G. A. Prinz, Magnetic properties of single-crystal Fe films grown on ZnSe epilayers by molecular-beam epitaxy, *J. Appl. Phys.* **61**, 3744 (1987).
52. J.-M. Jancu, R. Scholz, E. A. de Andrada e Silva and G. C. La Rocca, Atomistic spin-orbit coupling and k.p parameters in III-V semiconductors, *Phys. Rev. B* **72**, 193201 (2005).
53. O. Stier and D. Bimberg, Modeling of strained quantum wires using eight-band k·p theory, *Phys. Rev. B* **55**, 7726 (1997).
54. Y. Rajakarunanayake, R. H. Miles, G. Y. Wu and T. C. McGill, Band structure of ZnSe-ZnTe superlattices, *Phys. Rev. B* **37**, 10212 (1988).
55. M. Košuth, V. Popescu, H. Ebert and G. Bayreuther, Magnetic anisotropy of thin Fe films on GaAs, *Europhys. Lett.* **72**, 816 (2005).
56. A. T. Hindmarch, C. J. Kinane, M. MacKenzie, J. N. Chapman, M. Henini, D. Taylor, D. A. Arena, J. Dvorak, B. J. Hickey and C. H. Marrows, Interface induced uniaxial magnetic anisotropy in amorphous CoFeB films on AlGaAs(001), *Phys. Rev. Lett.* **100**, 117201 (2008).
57. A. F. Isakovic, J. Berezovsky, P. A. Crowell, L. C. Chen, D. M. Carr, B. D. Schultz and C. J. Palmstrom, Control of magnetic anisotropy in $Fe_{1-x}Co_x$ films on vicinal GaAs and $Sc_{1-y}Er_yAs$ surfaces, *J. Appl. Phys.* **89**, 6674 (2001).
58. J. A. Wolf, K. K. Anderson, E. D. Dahlberg, P. A. Crowell, L. C. Chen and C. J. Palmstrom, Tunable magnetization reversal in epitaxial bcc $Fe_{1-x}Co_x$ films on vicinal surfaces, *J. Appl. Phys.* **93**, 8256

(2003).
59. T. Yoo, S. Khym, H. Lee, S. Chung, S. Lee, X. Liu and J. K. Furdyna, Asymmetry in the planar Hall resistance of Fe films grown on vicinal GaAs substrates, *J. Appl. Phys.* **107**, 09C505 (2010).
60. W. Kipferl, M. Sperl, T. Hagler, R. Meier and G. Bayreuther, Stabilization of ferromagnetic order in epitaxial ultrathin Fe films, *J. Appl. Phys.* **97**, 10B313 (2005).
61. W. Kipferl, M. Dumm, P. Kotissek, F. Steinbauer and G. Bayreuther, Bloch's law for epitaxial ultrathin dot arrays with uniaxial magnetic anisotropy, *J. Appl. Phys.* **95**, 7417 (2004).
62. D. Niu, X. Zou, Y. Zhai, Z. Huang, I. Will, P. Wong, J. Wu and Y. Xu, Reduction of in-plane uniaxial magnetic anisotropy in patterned single-crystal Fe dot arrays, *IEEE Trans. Mag.* **45**, 3507 (2009).
63. K. K. Meng, J. Lu, S. L. Wang, H. J. Meng, J. H. Zhao, J. Misuraca, P. Xiong and S. von Molnar, Magnetic anisotropies of laterally confined structures of epitaxial Fe films on GaAs(001), *Appl. Phys. Lett.* **97**, 072503 (2010).
64. E. M. Kneedler, B. T. Jonker, P. M. Thibado, R. J. Wagner, B. V. Shanabrook and L. J. Whitman, Influence of substrate surface reconstruction on the growth and magnetic properties of Fe on GaAs(001), *Phys. Rev. B* **56**, 8163 (1997).
65. A. Ionescu, M. Tselepi, D. M. Gillingham, G. Wastlbauer, S. J. Steinmüller, H. E. Beere, D. A. Ritchie and J. A. C. Bland, Submonolayer growth of Fe on a GaAs(100)-2 $\times$ 6 reconstructed surface, *Phys. Rev. B* **72**, 125404 (2005).
66. D. M. Gillingham, M. Tselepi, A. Ionescu, S. J. Steinmuller, H. E. Beere, D. A. Ritchie and J. A. C. Bland, Smoothening of ultrathin Fe films grown on GaAs(100) observed by scanning tunneling microscopy and Brillouin light scattering, *Phys. Rev. B* **76**, 214412 (2007).
67. C. Godde, S. Noor, C. Urban and U. Köhler, Structural changes and alloying of annealed iron layers on GaAs(001) and GaAs(110), *Surf. Sci.* **602**, 3343 (2008).
68. S. Mirbt, B. Sanyal, C. Isheden and B. Johansson, First-principles calculations of Fe on GaAs(100), *Phys. Rev. B* **67**, 155421 (2003).
69. J. W. Freeland, I. Coulthard, W. Antel and A. P. J. Stampfl, Interface bonding for Fe thin films on GaAs surfaces of differing morphology, *Phys. Rev. B* **63**, 193301 (2001).
70. R. Moosbuhler, F. Bensch, M. Dumm and G. Bayreuther, Epitaxial Fe films on GaAs(001): does the substrate surface reconstruction affect the uniaxial magnetic anisotropy?, *J. Appl. Phys.* **91**, 8757 (2002).
71. E. Sjöstedt, L. Nordström, F. Gustavsson and O. Eriksson, Uniaxial magnetocrystalline anisotropy of metal/semiconductor interfaces: Fe/ZnSe(001), *Phys. Rev. Lett.* **89**, 267203 (2002).
72. J. M. LeBeau, Q. O. Hu, C. J. Palmstrom and S. Stemmer, Atomic structure of postgrowth annealed epitaxial Fe/(001)GaAs interfaces, *Appl. Phys. Lett.* **93**, 121909 (2008).
73. K. Olejnik, P. Wadley, J. A. Haigh, K. W. Edmonds, R. P. Campion, A. W. Rushforth, B. L. Gallagher, C. T. Foxon, T. Jungwirth, J. Wunderlich, S. S. Dhesi, S. A. Cavill, G. van der Laan and E. Arenholz, Exchange bias in a ferromagnetic semiconductor induced by a ferromagnetic metal: Fe/(Ga,Mn)As bilayer films studied by XMCD measurements and SQUID magnetometry, *Phys. Rev. B* **81**, 104402 (2010).
74. J. Tobin, S.-W. Yu, S. Morton, G. Waddill, J. Thompson, J. Neal, M. Spangenberg and T. Shen, Highly polarized emission in spin resolved photoelectron spectroscopy of α-Fe(001)/GaAs(001), *Surf. Sci.* **604**, 1342 (2010).
75. S. van Dijken, X. Jiang and S. S. P. Parkin, Room temperature operation of a high output current magnetic tunnel transistor, *Appl. Phys. Lett.* **80**, 3364 (2002).
76. X. Jiang, R. Wang, R. M. Shelby, R. M. Macfarlane, S. R. Bank, J. S. Harris and S. S. P. Parkin, Highly spin-polarized room-temperature tunnel injector for semiconductor spintronics using MgO(100), *Phys. Rev. Lett.* **94**, 056601 (2005).
77. J. M. Shaw, S. Lee and C. M. Falco, Overlayer-induced magnetic uniaxial anisotropy in nanoscale epitaxial Fe, *Phys. Rev. B* **73**, 094417 (2006).
78. L. Giovanelli, G. Panaccione, G. Rossi, M. Fabrizioli, C. S. Tian, P. L. Gastelois, J. Fujii and C. H. Back, Layer-selective spectroscopy of Fe/GaAs(001): influence of the interface on the magnetic properties, *Phys. Rev. B* **72**, 045221 (2005).
79. L. Giovanelli, G. Panaccione, G. Rossi, M. Fabrizioli, C. S. Tian, P. L. Gastelois, J. Fujii and C. H. Back, Interface magnetization profiling by X-ray magnetometry of marker impurities on Fe/GaAs(001)-(4$\times$6), *Appl. Phys. Lett.* **87**, 042506 (2005).
80. B. Kardasz, J. Zukrowski, O. Mosendz, M. Przybylski, B. Heinrich and J. Kirschner, Interface atomic structure and magnetic anisotropy in ultrathin Fe films grown by thermal deposition and pulsed laser deposition on GaAs(001), *J. Appl. Phys.* **101**, 09D110 (2007).
81. J.-M. Lee, J.-Y. Kim, S.-U. Yang, B.-G. Park, J.-H. Park, S.-J. Oh and J.-S. Kim, Magnetism of pristine Fe films on GaAs(100), *Phys. Rev. B* **76**, 052406 (2007).
82. T. Damm, M. Buchmeier, A. Schindler, D. E. Burgler, P. Grunberg and C. M. Schneider, Magnetic

properties of Fe films and Fe/Si/Fe trilayers grown on GaAs(001) and MgO(001) by ion-beam sputter epitaxy, *J. Appl. Phys.* **99**, 093905 (2006).
83. Z. L. Bao and K. L. Kavanagh, Epitaxial Fe/GaAs via electrochemistry, *J. Appl. Phys.* **98**, 066103 (2005).
84. E. B. Svedberg, J. J. Mallett, L. A. Bendersky, A. G. Roy, W. F. Egelhoff, Jr. and T. P. Moffat, A structural study of electrodeposited Fe on n-GaAs(001), *J. Electrochem. Soc.* **153**, C807 (2006).
85. K. Liu, D. Shen, J. Zhang, X. Wu, B. Li, B. Li, Y. Lu and X. Fan, MOCVD growth, structure and magnetic properties of Fe films grown on GaAs (001) substrates, *Sol. Stat. Comm.* **140**, 33 (2006).
86. A. T. Hindmarch, A. K. Suszka, M. MacKenzie, J. N. Chapman, M. Henini, D. Taylor, B. J. Hickey and C. H. Marrows, Structural and magnetic properties of magnetron sputtered $Co_{70}Fe_{30}$ films on GaAs(110), *J. Appl. Phys.* **105**, 073907 (2009).
87. A. T. Hindmarch, C. J. Kinane, C. H. Marrows, B. J. Hickey, M. Henini, D. Taylor, D. A. Arena and J. Dvorak, In-plane magnetic anisotropies of sputtered $Co_{0.7}Fe_{0.3}$ films on AlGaAs(001) spin light emitting diode heterostructures, *J. Appl. Phys.* **101**, 09D106 (2007).
88. J.-M. Lee, S.-J. Oh, K. J. Kim, S.-U. Yang, J.-H. Kim and J.-S. Kim, Kinetic stabilization of a pristine Fe film on (4×2)-GaAs(100), *Phys. Rev. B* **75**, 125421 (2007).
89. B. D. Schultz, N. Marom, D. Naveh, X. Lou, C. Adelmann, J. Strand, P. A. Crowell, L. Kronik and C. J. Palmstrøm, Spin injection across the Fe/GaAs interface: role of interfacial ordering, *Phys. Rev. B* **80**, 201309 (2009).
90. S. C. Erwin, S.-H. Lee and M. Scheffler, First-principles study of nucleation, growth, and interface structure of Fe/GaAs, *Phys. Rev. B* **65**, 205422 (2002).
91. D. O. Demchenko and A. Y. Liu, Influence of interface structure on electronic properties and Schottky barriers in Fe/GaAs magnetic junctions, *Phys. Rev. B* **73**, 115332 (2006).
92. P. Schieffer, A. Guivarc'h, C. Lallaizon, B. Lepine, D. Sebilleau, P. Turban and G. Jezequel, Formation of a body-centered-cubic Fe-based alloy at the Fe/GaAs(001) interface, *Appl. Phys. Lett.* **89**, 161923 (2006).
93. T. J. Zega, A. T. Hanbicki, S. C. Erwin, I. Zutic, G. Kioseoglou, C. H. Li, B. T. Jonker and S. R. M., Determination of interface atomic structure and its impact on spin transport using Z-contrast microscopy and density-functional theory, *Phys. Rev. Lett* **96**, 196101 (2006).
94. B. D. Schultz, C. Adelmann, X. Y. Dong, S. McKernan and C. J. Palmstrom, Phase formation in the thin film Fe/GaAs system, *Appl. Phys. Lett.* **92**, 091914 (2008).
95. Y. B. Xu, E. T. M. Kernohan, D. J. Freeland, A. Ercole, M. Tselepi and J. A. C. Bland, Evolution of the ferromagnetic phase of ultrathin Fe films grown on GaAs(100)-4×6, *Phys. Rev. B* **58**, 890 (1998).
96. J. S. Claydon, Y. B. Xu, M. Tselepi, J. A. C. Bland and G. van der Laan, Direct observation of a bulk-like spin moment at the Fe/GaAs(100)-4×6 interface, *Phys. Rev. Lett* **93**, 037206 (2004).
97. J. Stöhr, Exploring the microscopic origin of magnetic anisotropies with X-ray magnetic circular dichroism (XMCD) spectroscopy, *J. Magn. Magn. Mater.* **200**, 470 (1999).
98. J. F. Ankner and G. P. Felcher, Polarized-neutron reflectometry, *J. Magn. Magn. Mater.* **200**, 741 (1999).
99. P. Steadman, M. Ali, A. T. Hindmarch, C. H. Marrows, B. J. Hickey, S. Langridge, R. M. Dalgliesh and S. Foster, Exchange bias in spin-engineered double superlattices, *Phys. Rev. Lett.* **89**, 077201 (2002).
100. S. Park, M. R. Fitzsimmons, X. Y. Dong, B. D. Schultz and C. J. Palmstrøm, Magnetic degradation of an FeCo/GaAs interface, *Phys. Rev. B* **70**, 104406 (2004).
101. S. Park, M. R. Fitzsimmons, C. F. Majkrzak, B. D. Schultz and C. J. Palmstrøm, The influence of growth temperature and annealing on the magnetization depth profiles across ferromagnetic/semiconductor interfaces, *J. Appl. Phys.* **104**, 083905 (2008).
102. H. B. Zhao, D. Talbayev, Q. G. Yang, G. Lupke, A. T. Hanbicki, C. H. Li, O. M. J. van 't Erve, G. Kioseoglou and B. T. Jonker, Ultrafast magnetization dynamics of epitaxial Fe films on AlGaAs (001), *Appl. Phys. Lett.* **86**, 152512 (2005).
103. H. B. Zhao, D. Talbayev, G. Lupke, A. T. Hanbicki, C. H. Li and B. T. Jonker, Ultrafast interface magnetization dynamics in Fe/AlGaAs(001) heterostructure, *Appl. Phys. Lett.* **91**, 052111 (2007).
104. M. S. Blois Jr., Preparation of thin magnetic films and their properties, *J. Appl. Phys.* **26**, 975 (1955).
105. C. T. Chen, Y. U. Idzerda, H. J. Lin, N. V. Smith, G. Meigs, E. Chaban, G. H. Ho, E. Pellegrin and F. Sette, Experimental confirmation of the x-ray magnetic circular-dichroism sum-rules for iron and cobalt, *Phys. Rev. Lett* **75**, 152–155 (1995).
106. R. Richter and H. Eschrig, Spin-polarised electronic structure of disordered bcc FeCo alloys from LCAO-CPA, *J. Phys. F: Met. Phys.* **18**, 1813 (1988).
107. C. Andersson, B. Sanyal, O. Eriksson, L. Nordstrom, O. Karis, D. Arvanitis, T. Konishi, E. Holub-Krappe and J. H. Dunn, Influence of ligand states on the relationship between orbital moment and magnetocrystalline anisotropy, *Phys. Rev. Lett.*

99, 177207 (2007).
108. K. Nakamura, R. Shimabukuro, Y. Fujiwara, T. Akiyama, T. Ito and A. J. Freeman, Giant modification of the magnetocrystalline anisotropy in transition-metal monolayers by an external electric field, *Phys. Rev. Lett.* **102**, 187201 (2009).
109. K. Ohta, T. Maruyama, T. Nozaki, M. Shiraishi, T. Shinjo, Y. Suzuki, S.-S. Ha, C.-Y. You and W. Van Roy, Voltage control of in-plane magnetic anisotropy in ultrathin Fe/n-GaAs(001) Schottky junctions, *Appl. Phys. Lett.* **94**, 032501 (2009).
110. A. W. Rushforth, E. De Ranieri, J. Zemen, J. Wunderlich, K. W. Edmonds, C. S. King, E. Ahmad, R. P. Campion, C. T. Foxon, B. L. Gallagher, K. Výborný, J. Kučera and T. Jungwirth, Voltage control of magnetocrystalline anisotropy in ferromagnetic-semiconductor-piezoelectric hybrid structures, *Phys. Rev. B* **78**, 085314 (2008).
111. E. Villari, Change of magnetization by tension and by electric current, *Ann. Phys. Chem.* **126**, 87 (1865).
112. F. Nolting, D. Legut, J. Rusz, P. M. Oppeneer, G. Woltersdorf and C. H. Back, Anisotropy of the $L_{2,3}$ X-ray magnetic linear dichroism of Fe films on GaAs: Experiment and ab initio theory, *Phys. Rev. B* **82**, 184415 (2010).